PROVIDING PROPORTIONAL DIFFERENTIATION IN END-TO-END QUALITY-OF-SERVICE FOR WIRELESS MULTI-HOP AD HOC NETWORK

LI DAN

NATIONAL UNIVERSITY OF SINGAPORE

2005

PROVIDING PROPORTIONAL DIFFERENTIATION IN END-TO-END QUALITY-OF-SERVICE FOR WIRELESS MULTI-HOP AD HOC NETWORK

LI DAN

(*B.Eng, Xidian University, China*)

A THESIS SUBMITTED

FOR THE DEGREE OF MASTER OF ENGINEERING

DEPARTMENT OF ELECTRICAL & COMPUTER ENGINEERING

NATIONAL UNIVERSITY OF SINGAPORE

2005

To Mom, Dad and Elder Brother.

Acknowledgements

Firstly, I would like to express my deepest appreciation to my supervisor, Dr.Kong Peng-Yong. I am really grateful to him for incessantly and persuasively imparting me knowledge on doing research. I have benefited much from his valuable critiques and rigorous research attitudes. Without his continuous guidance and persistent help, this research would not have been possible.

Special thanks for Dr.Yin Qinghe kindly giving me many guidances on my research problems in the case that Dr.Kong Peng-Yong is unavailable.

Words alone cannot convey my gratefulness to my beloved parents and elder brother for their endless encouragement and selfless support all the time in my life. Especially, I dedicate this thesis to my deeply loved mom. Her great love to me through all of my life is the power to support me and the reason why I am willing to achieve more. I wish that what I did is able to bring her honors and happiness.

I also thank all of my colleagues and friends in Institute of Infocomm Research for giving me helps. Finally thanks for Institute of Infocomm Research and the National University of Singapore for granting me a research scholarship and providing the facilities.

Contents

List of Figures

List of Tables

Summary

Wireless multi-hop ad hoc networks suffer from time-varying network resources, limited power supply, dynamic topologies, etc. However, more and more applications which require quality of service (QoS) challenge the existing mechanisms of service provisions in wireless multi-hop ad hoc networks. Efficient resource allocations between different applications to satisfy as many users as possible in wireless ad hoc networks are really desirable.

This thesis proposes a general cross layer framework for wireless multi-hop ad hoc networks to support proportional differentiation in end-to-end QoS, which is able to achieve efficient network resource allocation via quantitative control on end-to-end QoS. In the framework, four mechanisms and three monitors in different layers of the protocol stacks adaptively cooperate via information exchanged between them so as to achieve the desired end-to-end QoS.

Based on the general framework, a specific realization called PDMED, is proposed based on a CSMA/CA medium access pattern to provide a consistent and accurate proportional differentiation on the average end-to-end packet delay. PDMED requires a distributed scheduler to adapt to the information from a QoS monitor and dynamically adjusts the contention window of a flow based on its instantaneous deviation from the maximum on normalized average end-to-end packet delay by weights among neigh-

boring flows. This is done such that a flow with a larger deviation from the maximum normalized delay is given a longer backoff duration to give way to transmissions from other flows with smaller deviations. PDMED has been extensively evaluated through random event simulations using OPNET. The results confirm that it is capable of providing a consistent and accurate proportional differentiation in end-to-end packet delay, which is otherwise not achievable under various traffic conditions. A benchmark against the IEEE802.11e using video traces shows that PDMED is significantly more flexible in providing an accurate and controllable end-to-end proportional differentiation.

In order to improve the performance of PDMED in wireless multi-hop ad hoc networks, A improvement, called PDMED+ has been also proposed. Based on the finding of self-similar characteristic in signal-to-noise ratio (SINR) under the random waypoint mobility model, PDMED+ utilizes the predicted SINR to increase efficiency of channel utilization so as to improve the total throughput of the network with the condition of maintaining the proportional differentiation on average end-to-end delay. Conceptually, PDMED+ predicts whether the head of line (HOL) packet will be successfully transmitted firstly. Then if the transmission will not be successful, PDMED+ adjusts the transmission time of the packet to the time when the channel quality becomes good for a successful packet transmission, so as to avoid occupancy of wireless channels by unsuccessful transmissions and to transmit the packet as soon as good channel quality is available. Random event simulations has also been conducted to evaluate the performance of PDMED+ using OPNET. The evaluation results exhibit that PDMED+ is capable of increasing the total throughput of the network when providing an accurate proportional differentiation on average end-to-end delay.

Chapter 1

Introduction

1.1 Challenge of QoS Provision in Wireless Multi-Hop Ad hoc Network

These days, wireless networks have become increasingly popular in the network industry. They can provide mobile users with ubiquitous communication capability and information access regardless of locations. However, conventional wireless networks are often connected to a wired network and require a fixed wire-line backbone infrastructure. All mobile hosts in a communication cell can reach a base station on the wired network in one hop radio transmission. In parallel with the conventional wireless networks, another type of wireless network model, based on radio to radio multi-hopping, has neither fixed base stations nor a wired backbone infrastructure. This kind of network is called wireless ad hoc network. For example, without specifying any application, wireless sensor networks [1], wireless multi-hop hotspots LAN can be generally considered as such kind of networks in network infrastructure, constituted of mobile nodes which act as both mobile hosts and mobile routers. So wireless ad hoc network is expected to play an important role in civilian and military forums in future.

Naturally a wireless ad hoc network is an autonomous system of mobile routers (and associated hosts) connected by wireless links — the union of which form on an arbitrary graph. The routers are free to move randomly and organize themselves arbitrarily; thus, the network's wireless topology may change rapidly and unpredictably. Such a network may operate in a stand-alone fashion, or may be connected to the larger Internet [2].

Being self-organized and not relying on existing infrastructure, wireless ad hoc networks have several salient and unique features [3]. First, their topologies are dynamic and change often rapidly because of unpredictable and arbitrary movement of nodes. Thus, node inter-connectivity and link properties such as capacity and bit error rate cannot be predetermined. Next, the transmission medium has a bandwidth-constrained and time-varying capacity because of unstable wireless link. In addition, distance between the ends of the link, obstacles in the environment, externally generated noise and interference caused by other transmissions also make the capacity of the wireless communication be reduced and apt to be highly variable. Finally, wireless ad hoc networks are only able to support power-constrained operation because of lightweight batteries to support portability. The limited power supply constrains the transmission range, data rate, communication activity and processing speed of the devices. Without centralized administration, distributed operations on every node are also important characteristics of wireless ad hoc networks.

In spite that above mentioned features of wireless ad hoc networks make the networks with less resources and vulnerable for operations, because of rising popularity of multimedia applications and potential commercial usage of wireless ad hoc networks, data with different requirements of timely delivery are needed to be supported in a network. Thus, quality of Service (QoS) support in wireless ad hoc networks has become an

unavoidable task. For example, real-time image information requires to be delivered immediately so that the image of illegal intruder can be detected and help guards take action promptly. However, measured temperature data can be delivered with some delay, such as 5 minutes, to the control center for processing.

However, the vulnerable, highly time-varying and limited resources of wireless ad hoc network make it have limited capacity to satisfy the delivery requirements of users' applications. Therefore, the network resource should be allocated between applications in an efficient way, i.e. trying the best to satisfy as many users as possible. We think that a quantitatively balanced network resource allocation between applications based on their QoS performances is the way to achieve this objective.

1.2 Motivation

Having insight of "tune knob" feature of proportional differentiation model to quantitatively control service spacings between users, we think that this feature is desirable for efficient network resources allocation between QoS requirements of users. Using this function, we can delicately adjust the resource allocations between flows so as to achieve an optimized situation. Suppose that there are two real-time video flows that both expect 0.05 second as the maximum of end-to-end packet delay. If a packet is unable to reach destination before the deadline time, the packet may be dropped. And two flows are able to tolerate the packet drop ratios with 0.01 and 0.05 respectively. The flow with 0.01 drop ratio has higher priority, whereas the other has lower priority. When the network resource is so limited that if we allocate network resource to higher priority flow first to guarantee its requirement (thus its drop ratio is 0), the drop ratio of lower priority flow will be over 0.05, such as 0.06. And, if the higher priority flow is allocated less resource such that its drop ratio becomes 0.01, the lower priority flow

will get more resource such that its drop ratio can be reduced to 0.05. In this situation, guaranteed service and relative differentiation methods sacrifice the lower priority flow in order to satisfy the higher priority flow. Service assurance methods alternatively try to satisfy one flow if its requirement is not satisfied. All of these ways are unable to quantitatively control the resource allocation so as to keep the network in optimized situation, i.e. 0.01 drop ratio for higher priority flow and 0.05 drop ratio for lower priority flow. However, if using "tune knob" function in proportional differentiation QoS provisioning, we may quantitatively set the ratio between the drop ratios of two flows and allocate the network resource aiming to achieve the ratio on end-to-end QoS of two flows. Thus, the optimized solution with 0.01 and 0.05 drop ratios on higher and lower priority traffics respectively can be achieved.

In the literature, we learned that there are numerous mechanisms across the protocol layers and time scales for QoS delivery in multi-hop ad hoc networks. Among these mechanisms are QoS routing protocols, admission control policies, resource reservation schemes, packet scheduling algorithms, QoS capable MAC protocols, etc., as investigated in Chapter 2. Unfortunately, none of these existing mechanisms is alone capable of providing satisfactory end-to-end proportional differentiations over multi-hop scenarios. Although some works have implemented the proportional differentiation model over one-hop behavior, time-varying topology and wireless medium's capacity of ad hoc network spoil accurate quantitative differentiation after transmissions through multiple hops. Therefore, the "tune knob" function to control the service quality spacing among users is unable to achieve so as to lose the significance of implementing proportional differentiation model. Thus, it is significant to research on a mechanism to allocate network resources between users with proportionally differentiated control on their end-to-end QoS performances.

In addition, mobility of nodes and time-varying wireless channel are factors that greatly affect the network capacity in wireless multi-hop ad hoc network. Usually, the existing methods either provide service assurance on end-to-end QoS, which only allocates available network resources to users according to their priority order without caring about the quantitative end-to-end performance of the traffics of every user, or provides guaranteed service which ignores quantitative variation of network capacity because it only admits the traffics into network whose requirements of network resources in total are definitely below the minimum network capacity. Thus, these methods do not need to particularly handle the effects generated by mobility of nodes and time-varying channel because these factors won't destroy their QoS goals. However, in order to increase the efficiency of the network resource utilization while providing proportional differentiation on end-to-end QoS, the effects on end-to-end QoS of flows generated by mobility of nodes and channel variation cannot be ignored and have to be handled quantitatively.

In wireless multi-hop ad hoc networks, movement of nodes may lead to variation of signal strength and interference strength from other simultaneous transmissions in networks and link breakage. Thus, movement of nodes generates both errors on packet transmission due to variation on wireless link transmission and delay overhead due to re-routing process intrigued by link breakage. In addition, in CSMA/CA based networks, the wireless medium is shared by nodes in a distributed pattern. Because of the broadcasting feature of wireless channels in ad hoc networks, interference is a factor largely affecting variation in wireless channels, compared to other noise factors in wireless medium environments. Thus, mobility of nodes also generate time-variation of wireless channel in CSMA/CA based wireless multi-hop ad hoc networks. In order to achieve proportional differentiation in end-to-end QoS in the environment with

mobility of nodes and time-varying wireless channel, a scheme to detect the effects on packet transmissions due to mobility of nodes is necessary. After surveying research works in the literature that studied variation of wireless channels or mobility of nodes for improving the network performance, they either intensively analyzed time-varying characteristic of wireless channel and its effects on packet transmissions in cellular networks, or achieved good algorithms to track mobility of nodes in order to improve hand-over and routing performance, etc. None of the existing works studied the effects of mobility of nodes on packet transmissions in wireless multi-hop ad hoc networks based on CSMA/CA access protocol.

In addition, from the motivations above, it is obvious that a combination of several mechanisms with different network functions have to work collaboratively to achieve our QoS goal. For example, we may need a packet scheduling algorithm that transforms the QoS requirements into medium access priorities and works with a MAC protocol that provides the multiple priorities. Also, we need a channel monitor capturing the instantaneous channel quality so as to compensate its negative effects on the QoS schemes. Therefore, a framework in which different mechanisms relying on different protocol stacks are able to collaborate together with the purpose of providing proportional differentiation on end-to-end QoS is also desirable.

1.3 Contribution and Organization of the Thesis

This thesis first contributes in developing a cross layer framework for end-to-end proportional differentiation in wireless multi-hop ad hoc networks. While it is designed with proportional differentiation in mind, we realize that the framework is also applicable to achieve other general QoS requirements. With the framework, the thesis also contributes a specified realization called Proportionally Differentiated Multi-hop

End-to-end Packet Delay (PDMED), which is evaluated through simulations. The simulation results indicate that an accurate end-to-end proportional differentiation across multi-hop ad hoc network which cannot be achieved otherwise, can now be achieved.

This thesis also discovers self-similar characteristics of signal-to-noise ratio in CSMA/CA based wireless multi-hop ad hoc network with the condition that nodes move under random waypoint model. Cooperating with a method to forecast the channel quality based on observed self-similar characteristic in signal-to-noise ratio, the thesis further suggests an improvement to the proposed realization called PDMED+, which is verified by random event simulations to be able to achieve proportional end-to-end differentiation in the environment with node mobility and channel variation and also increase the total end-to-end throughput of the whole network.

The remainder of the thesis is organized as follows. In Chapter 2, we give the literature review on the existing methods and mechanisms for QoS provisioning in multi-hop ad hoc networks and for handling channel variation and mobility in wireless networks. Chapter 3 presents the cross layer framework and PDMED to provide accurate proportional differentiation in multi-hop ad hoc networks. The performance is evaluated via simulations. Chapter 4 proposes a method to predicting signal-to-noise ratio of packet transmissions due to nodes mobility and channel errors and the improved scheme (PDMED+). Performance is also evaluated by simulations. Chapter 5 concludes the thesis and points out future research directions.

Chapter 2

Literature Review

2.1 QoS Provision by Resource Allocation in Wireless Ad Hoc Networks

In the literature, a large number of research activities on QoS support in MANETs have been done, including QoS models, QoS resource reservation signaling, admission control, QoS routing and QoS medium access control (MAC), etc. They did a lot of endeavors to realize various kinds of QoS support. With our motivation, we intensively studied the mechanisms that allocate different network resources to different applications in a wireless ad hoc network. Basically, according to the QoS goals they achieved, we classified the studied mechanisms in four categories: guaranteed services, relative differentiation, proportional differentiation and QoS over multiple hops.

2.1.1 Guaranteed Services

In order to provide different guaranteed QoS to different types of applications, various distributed MAC protocols have been proposed in the literatures. Specifically, these MAC protocols can provide different upper bounds in packet access delay. For example,

([4],[5]) propose distributed TDMA protocols that can guarantee at least one collision free time slot for each node in a given duration. This guarantee is possible in the absence of a central controller by using discrete mathematics mapping function to pseudo-randomly arrange the transmission and reception at each node. In the same spirit of bounding access delay, [6] proposes a distributed CSMA/CA MAC protocol that can guarantee access to a node by emulating a round robin algorithm. This round robin algorithm is enforced by making each node to send a Black Burst, i.e., pulses of energy at the end of back-off and the duration of Black-Burst is proportional to the packet access delay. The node can only transmit its packet if the channel remains idle after its Black-Burst. Otherwise, the node has to perform another back-off which will increase the duration of its Black-Burst.

While the two MAC protocols above are capable of providing guaranteed QoS in a distributed wireless ad hoc network, some forms of resource reservation are required. Due to unpredictable capacity, the reservation often means resource over-provisioning and thus makes the guaranteed QoS not scalable and efficient. Compared to guaranteed QoS, differentiated QoS is not to deliver a hard assurance in the perceived performance but to give different resources to different flows such that different levels of performance can potentially be achieved at the flows. This flexibility of differentiated QoS makes it suitable for wireless ad hoc network with volatile capacity.

2.1.2 Relative Differentiation

As a mechanism to provide differentiated QoS, prioritized channel access has been extensively studied. In [7], a MAC protocol is proposed such that different priorities are achieved by assigning different fixed Black-Burst durations to different traffic classes. Within a priority class, a randomized initialization protocol is used to enforce

a round robin sequence of transmissions among distributed nodes so that collision can be avoided. While Black-Burst is indeed a practical method to achieve prioritization, the priority is only local among all nodes within the region of one hop where there is no hidden node. In the presence of hidden nodes, high priority node may be marginalized compared to a node with lower priority. Hence, [8] proposes to tackle this mis-scheduling problem among all nodes within a region of two hops. According to [8] before sending a Black-Burst at the end of a back-off, the high priority node sends a busy tone which will be echoed by its receiver. All low priority nodes that hear the busy tone defer their transmissions.

Compared to Black-Burst, differentiating back-off duration is another technique in providing different priorities. This technique has been adopted in [9] to provide QoS differentiation in IEEE 802.11 where a higher priority node has a shorter back-off duration. It has been shown that this technique does not work well in a noisy environment with prevalent propagation impairments. Also, a shorter back-off duration cannot really provide a higher priority to TCP flow where its throughput is measured on an end-to-end basis. Under these conditions, [9] indicates that a better differentiation can be achieved by using a shorter distributed inter-frame spacing(DIFS) duration, instead of back-off duration for a higher priority node. This finding has also been reported in [10]. Further, [10] reveals that, while a combination of back-off duration and DIFS duration can provide good QoS differentiation, the differentiation can be dramatically affected by channel condition and number of active nodes. Specifically, when the number of nodes is large, an accurate differentiation is harder to achieve by merely controlling the back-off duration because of more frequent transmission collisions. On the other hand, with a smaller number of nodes, adjusting only DIFS duration is not efficient in achieving the desired differentiation due to a waste of transmission times.

In view of the individual deficiencies of both back-off duration and DIFS duration techniques, IEEE 802.11 working group has taken the effort to define a standard mechanism to use them collectively to achieve efficient QoS differentiations [11]. The effort yields 802.11e which has been extensively studied in the literatures ([12],[13]). From the studies, controlling back-off duration is effective in introducing throughput differentiation while adjusting DIFS duration amplifies the differentiation. The studies also show that 802.11e can provide differentiation when there is a fixed number of active nodes within a radio range in an idealistic channel even though the traffic load is at a saturated level. However, the differentiation is vulnerable to changes in the number of nodes and traffic load. This vulnerability is partly due to the definition of its differentiation where a flow can choose one amongst a small number of service classes (or priorities) that best meet its QoS requirement, based on the assurance that the perceived QoS of higher classes will be better, or at least no worse that that of lower classes. This type of differentiation is called relative differentiation compared to proportional differentiation which offers predictable and controllable differentiations between different service classes [14].

2.1.3 Proportional Differentiation

A simple form of proportional differentiation in throughput has been termed fairness. Let g_i and ϕ_i be respectively the throughput and proportional differentiation parameter for node i. Then, unfairness may be expressed as follows:

$$\bar{\mathcal{F}} = \max_{\forall i,j} \left\{ |\frac{g_i}{\phi_i} - \frac{g_j}{\phi_j}| \right\} \tag{2.1}$$

where a smaller $\bar{\mathcal{F}}$ means a better fairness. In order to achieve good fairness, [15] has proposed a distributed fair MAC protocol to ensure a minimum fair share of medium to a node while maximizing the spatial channel reuse for throughput improvement.

This is achieved by mapping the virtual clock of weighted fair queuing into the back-off duration of a contending node and by allowing a lookahead window in the range of virtual clock eligible for service. While [15] uses weighted fair queuing, similar works in achieving fairness by mapping virtual clock of other fair queuing models, such as start time fair queuing and worst-case-fair fair queuing, into back-off duration have been reported in ([16],[17],[18],[19]). Unfortunately, all these works can only achieve proportional differentiation (fairness) locally or globally between two nodes over one hop. With multiple hops in a wireless network, we argue that the proportional differentiations should be achieved in an end-to-end manner across all hops but not limited to a concatenation of local proportional differentiations at each hop.

2.1.4 QoS over Multiple Hops

In order to provide QoS across multiple hops, [20] has proposed a distributed packet scheduling algorithm for CSMA/CA based MAC protocols to achieve an accurate transmission order as if in a centralized scheduler that provides QoS differentiation. Based on the desired transmission order, the scheduling algorithm assigns to every packet an appropriate priority. With the priority of a head packet, each node can rank itself against all its neighboring nodes after overhearing their head packets' priorities which are piggy-backed on other transmissions. According to the rank, a node will determine its back-off duration to achieve the desired transmission order. Although the algorithm is capable of ensuring an accurate transmission order in a multi-hop setting, it is for packet and not flow. Further, there is no end-to-end QoS across multiple hops.

To provide to a flow an end-to-end QoS across multiple hops, [21] has proposed a simple modification to CSMA/CA MAC protocol so that DATA and ACK frames will carry piggy-backed channel reservation for the next transmission and thus, no RTS/CTS ex-

change is required except for the first packet of a traffic burst at the first hop. As such, as long as the first DATA frame manages to acquire the channel at the first hop, the subsequent packets are guaranteed channel access without further reservation delay in the absence of channel error. This scheme is able to provide a better QoS to a real-time flow, compared to a best-effort flow along a multi-hop path. However, it is not easy to support multiple real-time flows at a same time, especially when the different real-time flow have different QoS requirements.

In an effort to provide different QoS to different flows across multiple hops, [22] proposes a coordinated multi-hop packet scheduling algorithm that requires some modifications to and co-operations from the CSMA/CA MAC protocol. In [22], the end-to-end QoS requirement of a flow is transformed into an instantaneous priority by the packet scheduling algorithm. Here, a packet that has not been offered sufficient service in the previous hop will be given a higher priority in the future hops and vice versa. The priority of the current and the next packets will be piggy-backed onto RTS/CTS and DATA/ACK packets, respectively. Hence, all nodes within a hop know each other's instantaneous priorities and only the node with the highest relative priority will contend for the channel while the other nodes defer their transmissions. It is the mechanism of adjusting a packet's priority at a hop based on its experience in previous hops that enables end-to-end QoS across multiple hops. However, it is obvious that the opportunities of compensating a packet in downstream hops is limited by the number of downstream hops and the competition situations in downstream hops. These limitations make this scheme only capable of providing coarse QoS provision.

In order to have more adjustment space for QoS provision, Reference [23, 24] proposed DCS-NPDD-MAPS framework to adjust network access for a packet of a flow according to the end-to-end performance of previous packets so as to compensate to the previ-

ous bias resource allocation promptly and achieve end-to-end assurances in multi-hop wireless networks. In the framework, Dynamic Class Selection (DCS) gives a way to dynamically choose the priority for flows according to their instant end-to-end performances. Neighborhood Proportional Delay Differentiation (NPDD) scheduler ensures to differently allocate the access of the medium resources in a proportional ratio in queuing delay between flows in a node according to their priority. Medium Access Priority Selection (MAPS) supports the priority order of packets of flows in a contending area in MAC layer. IEEE 802.11e is used to realize the priority in competing to access the medium. These algorithms also achieve end-to-end service assurance for flows via mapping end-to-end QoS targets into priority indexes. This similar service compensation mechanism has been adopted by [25] for the same goal. More aggressively, [25] intends to provide a guarantee in end-to-end packet delay through admission control. Since there is no intuitive way to compute the capacity of a multi-hop ad hoc network, the admission control is done using an admit-then-test method. Specifically, a flow with end-to-end delay requirement is first admitted and then, its impact on the channel idle time is monitored. If the idle time becomes too short as a result of the new flow, another flow that has no end-to-end delay requirement is selected for rejection.

2.1.5 Summary

Among all above schemes which provide various forms of QoS in wireless ad hoc network, we found that none of them is capable to supporting the proportional differentiations in end-to-end QoS. We intensively studied the schemes that either adopt proportional differentiation model or provide end-to-end QoS over multiple hops in order to investigate their potentials of providing proportional differentiation in end-to-end QoS. We summarized the results in Table 2.1. The table shows the QoS goals of

Ref.	QoS Goals	Methods	Problems
[18] [19]	Accurate fairness of network resources between every node in the network.	1)Approximate STFQ via setting appropriate back off time. 2)Using round number to control accuracy of fairness.	One hop fairness. Cannot support end-to-end QoS of flows with multiple hops.
[20]	Fairness according to an ideal scheduling algorithm in multi-hop network.	1)Priority medium access(Non-persistent CSMA/CA): hearing priorities from neighbor nodes. Priority access to the node with the highest priority.	Cannot support end-to-end QoS of flows with multiple hops.
[21]	Guaranteed service for a real-time flow over multi-hop networks.	Piggy-backing channel reservation on DATA/ACK frames.	Reserving network resource completely for a flow cannot support multiple flows with diverse QoS requirements.
[22]	Service assurances for flows in multi-hop network.	1)Priority medium access: hearing priorities from neighbor nodes. Priority access to the node with the highest priority. 2)Coordination mechanisms to adjust priority of packets in downstream hops.	Coarse QoS with quantitative control.
[23] [24]	Service assurance of flows in multi-hop wireless networks.	DCS-NPDD-MAPS framework. 1)Dynamically adjust flows' priorities according end-to-end performances. 2)proportional queuing delay between neighbors. 3)IEEE 802.11e for prioritized medium access.	Unable to quantitatively control the network resources between flows.
[25]	Guarantee services flows in multi-hop wireless networks.	1)Partitioning end-to-end requirement into a single hop. Adjust contention windows according to the performance of satisfying the requirement in previous packets. 2)Admission control of low-priority traffics via monitoring congestion of channel.	Unable to quantitatively control network resource allocation between flows. Sacrificing low-priority flows to guarantee high-priority cannot efficiently utilize network resources

Table 2.1: Problems of existing schemes for providing proportional differentiation in end-to-end QoS

the studied schemes, their methods and the problems that they may suffer if providing proportional differentiation in end-to-end QoS. Conclusively, the main problems are: 1) Only providing guaranteed service, prioritized access, proportional differentiation over one hop is unable to provide proportional differentiation over multi-hop in wireless multi-hop ad hoc networks. A coordinated method to support proportional differentiation over multiple hops is necessary. 2) A support which merges end-to-end QoS of every flow into medium access protocols on every hop is a must. 3) Too strict

QoS provision methods, such as strict prioritized access or guaranteed service may reduce the number of QoS-expected flows supported, and are not desirable for efficient utilization of network resources allocation.

2.2 Mobility and Channel Variation in Wireless Networks

Mobility and wireless channel variation are factors greatly affecting the performance in physical layer. Both mobility and wireless channel variation generate errors in transmitting packets. Mobility also lead to link breakage. In order to support the performance of upper layer, such as scheduling and routing, a QoS support method in physical layer to capture the effects on packet transmission due to nodes' mobility and time-varying wireless channel is necessary to cooperate to QoS provision scheme in in wireless multi-hop ad hoc networks.

2.2.1 Channel Characteristic and Prediction

Because channel quality directly reflects whether a transmission is successful or not, some of work have been done to model and predict the channel quality in wireless environment. Some methods have been proposed to predict the signal using statistic characteristic methods. Reference [26] proposed a decision-directed channel predictor for orthogonal frequency-division multiplexing (OFDM) communications over time-varying channels. Basically, this method uses demodulated receive data to yield an minimum mean-square error(MMSE) predictor so as to get up-to-date channel state information for decoding and equalization. This method is an estimation way, based on characteristic of OFDM systems. Reference [27] proposed a prediction method for forecasting the fractal signal strength based on the fact that the signal strength exhibits self-similar characteristic over sea clutters. This method is able to predict

the future signal strength through the parameter, the Hurst Parameter, reflecting the long-range dependent characteristic. However, above methods are based on the case that communication is carried over the separate channel completely used by for a user. Thus, these methods capture the continous characteristic of wireless link of a user.

In order to predict the instantaneous channel quality in scenario that several users share a wireless link by different time slots, [28] proposed a pilot-based scheme to detect the channel state in wireless networks with a centralized control on transmissions. Through probing the channel via pilot packet to collect information about channel status, the duration of channel being good or bad for transmissions is able to be estimated and constructed. The results benefit for packet scheduling so as to improve QoS provision and network performance. But, this scheme is used for cellular networks with a central controller for packets from several users. It is difficult to use in multi-hop ad hoc networks. Thus, the interference effect on wireless link due to transmissions of nearby nodes that exists in multi-hop ad hoc networks cannot be handled by this method.

2.2.2 Mobility Tracking and Prediction

Because mobility is a key factor that affects wireless channel in wireless ad hoc network, in literatures some works have been done to handle the mobility of nodes in order to improve QoS provision in wireless networks. [29] proposed a hierarchical mobility model to catch the characteristics of the mobile nodes' movement and a hierarchical location prediction algorithm to improve hand-offs, relieve congestion, etc., so as to improve QoS provision cooperated with reservation and routing protocols in wireless ATM networks. The main features of this scheme is two-level mobility model for nodes movement, cell location and movement trajectory in a cell, and two-level location prediction, global prediction for cell location and local prediction for movement in a cell for

a node. For global prediction, the authors proposed an approximate pattern matching algorithm to abstract the geometric similarity between two cell sequences to predict which cell is a node located. For local prediction, the authors tracked trajectory of a node and used an extended self-learning Kalman filter to predict its movement in a cell. Although this scheme is able to predict the location of a mobile node specifically, the two hierarchical prediction is complex for implementation. [30] also proposed a prediction scheme which is much simpler. This scheme predict the probabilities that a mobile node will be active in nearby cells in DS/CDMA wireless network so as to help resources reservation and achieve maximum resource utilization. Adaptive fuzzy inference approach is used to estimate the mobility information based on the real-time measurements of received pilot signal power. A recursive least square algorithm undertake prediction for probability of moving to neighbor cells of a node in next moment. However, both of above two schemes are based on cellular networks with support of base stations. They are difficult to be implemented in mobile ad hoc networks.

In order to solve the problem of node positioning in ad hoc networks, a infrastructure-free positioning and distributed algorithm that does not rely on GPS (Global Positioning System) is proposed in [31]. This scheme is to build a relative coordinate system for a node using the distances between this node and other nodes in the networks so as to find its own location compared to other neighbor nodes. Through choosing several nodes to form the Location Reference Group, all of nodes in the network adjust their local coordinate systems consistently so as to locate their own positions in the networks. Indeed, the accuracy and stability of this scheme are much dependent on stability of Location Reference Group formed by several nodes. If the movement of these nodes is fast and dynamic, it is hard to compute the correct location in the network for a node. And, this scheme provides only position information. Although it is able to reflect

movement of nodes, which is able to give information for routing protocols, it is not sufficient to show the transmission channel quality due to mobility of nodes, especially the variation of signal strength and interference strength generated by movements of nodes in networks.

2.2.3 Interference Estimation

Reference [32] proposed a model to calculate interference levels in wireless multi-hop ad hoc networks. This model is based on honey-grid lattice to capture the expected value of carrier-to-interference ratio by taking into account the number of nodes, density of nodes, radio propagation aspects, the amount of relay traffic and multi-hop characteristic in multi-hop ad hoc networks. This work is able to reflect the effects of variations in network size, network density and traffic load on carrier-to-interference ratio generally. However, it is unable to give us the instantaneous carrier-to-interference, which is determined by movement pattern of nodes in networks.

2.2.4 Summary

In wireless multi-hop ad hoc networks with CSMA/CA access protocols, mobility of nodes is a key factor which dramatically affects the network performance in routing and packet transmission. The factor varies signal strength and the wireless transmission environment due to interferences, increases errors in transmitting packets and even breaks the transmission links. Therefore, the transmission time of a packet and whether a packet is transmitted successfully both are affected by mobility of nodes.

From above investigations, none of existing works provides a way to capture the characteristic of the effects on packet transmissions due to mobility of nodes and broadcasting wireless mediums in wireless multi-hop ad hoc networks based on CSMA/CA access

protocol. Thus, it is significant to study on the effect on packet transmissions due to mobility of nodes in CSMA/CA based wireless multi-hop ad hoc networks.

Chapter 3

Cross Layer Framework for Proportional Differentiation in End-to-end QoS and a Realization Scheme

3.1 Introduction

In chapter 2, we have found that only one component in ad hoc networks is difficult to provide proportional differentiation on end-to-end QoS among flows. In this chapter, we propose a cross layer framework for end-to-end QoS in wireless multi-hop ad hoc networks and contribute a realization of the framework to achieve an accurate proportional differentiation on average end-to-end packet delay among flows in a network.

The remainder of this chapter is organized as follows. First, we will present the network model and problem statement. Next, we propose a cross layer framework for providing end-to-end proportional differentiation in multi-hop ad hoc networks. Then, we give a

realization of the framework, PDMED. Finally, we evaluate PDMED through random event simulations. The conclusion is given in the end of the chapter.

3.2 The Network Model and Problem Statement

We consider a multi-hop wireless network without access points for infrastructure networks. Nodes enter or leave the network at will. They move around in a geographic area. Any user can host applications towards other users via some nodes as intermediate routers. Thus, all users form connections of a path with one or multiple hops to another node (destination) with the underlying routing protocol. The medium access for each node is based on content-based protocol (CSMA/CA). We focus on a multi-hop scenario. Not all users are within each other's transmission and carrier sensing range. In this network, the end-to-end QoS proportional differentiation problem is formulated as follows:

Applications at any node request their packets to be transmitted to another node that is not in the transmission and carrier sensing range of the source node. The network is able to provide services in the quality spacing of the end-to-end metrics between the applications according to a proportional ratio.

3.3 Introduction of Cross Layer Framework

As illustrated in Fig. 3.1, the framework consists of four mechanisms, namely traffic policing, centralized scheduler, distributed scheduler and admission control. These mechanisms in turn are assisted by three monitors, namely QoS monitor, route monitor and channel monitor. We will next describe these mechanisms and monitors as well as explain the interactions among them.

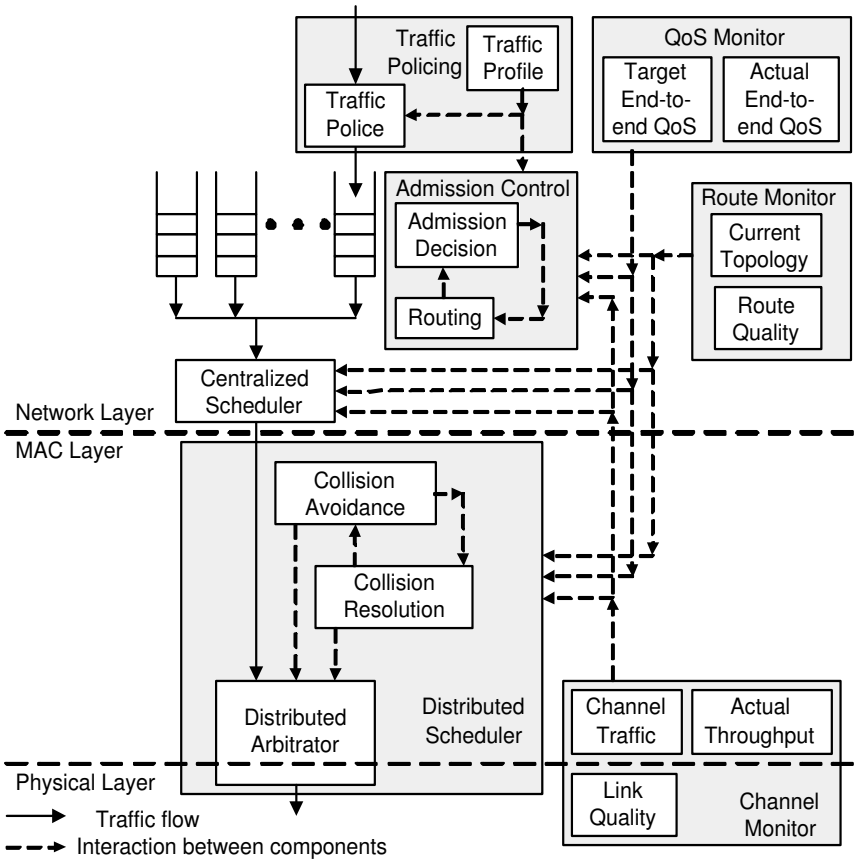

Figure 3.1: Cross layer framework for proportional end-to-end QoS in wireless multi-hop ad hoc networks

In Fig. 3.1, the traffic policing is to ensure that the traffic arrival of a flow is in accordance to the declared traffic profile. For the arrived packets that have exceeded the profile, the traffic police will either discard them or mark them so the marked traffic can be discriminated when the need arises later.

The traffic profile component of traffic policing is also used in the other mechanism, i.e., admission control. Generally, admission control needs to derive the resource requirement of a flow based on the traffic profile before deciding if the flow should be admitted into the system. Normally, the flow is admitted only when the required resource is not more than the available resource in a route. Thus, routing is an integral part of the admission control and directly affects the admission decision. The failure

of admitting a flow to a route will prompt the routing component to search for another route before submitting the flow for admission decision again in an iterative approach. Despite rejecting a flow on a route due to insufficient resource, the available resource is not always known with certainty at the time of making admission decision. This is due to the time-varying characteristics of link quality which also affects the instantaneous actual end-to-end QoS and quality of a route. Thus, the admission control in the proposed framework needs to provide for and dynamically evaluate the impacts of the time-varying factors. As such, when the current route becomes unusable to a flow, the routing component may dynamically re-route the flow to another route that meets the flow's original performance requirements.

In order to dynamically evaluate the time-varying characteristics, the framework uses a channel monitor, a route monitor and a QoS monitor. The channel monitor spans across both physical and MAC layers. In the physical layer, the channel monitor measures the link quality. In the literature, the link quality can be given in terms of bit error rate, received signal strength, signal to noise and interference ratio, etc. In the MAC layer, the channel monitor keeps track of the actual throughput as well as the channel traffic. In the framework, channel traffic is a general term which includes all received packets. It is based on these received packets which may be erroneous or error free that other components in the framework may derive various information, such as the traffic load, actual QoS, current topology, etc.

Different from channel monitor which spans across the lowest two protocol layers, route monitor appears only in the network layer. Here, route monitor may quantify the route quality in terms of the effective end-to-end bit error rate, remaining time to a broken route, etc. Hence, the route quality is determined partly based on the mobility information and the qualities of its component links which can be provided, among others

by the channel monitor. In the proposed framework, the route monitor also keeps track of the current topology which can be affected by mobility.

Similar to the route monitor, QoS monitor is in the network layer where the actual end-to-end QoS can be measured. The actual QoS can be compared against the target QoS where an obvious difference suggests a failure in meeting performance requirement and thus, triggers a sequence of activities in various mechanisms, such as re-routing and adjustments in transmission schedule.

Thus far, we have described the traffic policing and admission control, which are two mechanisms working on different time scales. Specifically, traffic police must make a policing decision on each newly arrived packet while the admission control needs to decide on re-routing only after a sufficiently large number of packet has been transmitted or monitored such that the statistics collected by all the monitors are meaningful. Now, we introduce another mechanism, i.e., the centralized scheduler will decide among a set of the local flows, which to serve after considering inputs from all the monitors. For example, while making decision, the centralized scheduler needs to consider the target and actual end-to-end QoS of a flow that are provided by the QoS monitor.

In the centralized scheduler, the chosen flow will have its head packet sent from the network layer to its distributed scheduler in the MAC layer. Here, the distributed scheduler will decide which one from a set of neighboring nodes, should transmit its packet to physical medium using what parameters. These parameters which include but not limited to modulation scheme, carrier frequency, transmission power, packet length, etc., are decided by the distributed arbitrator, i.e., a component of the distributed scheduler. Note that the distributed arbitrator spans across two protocol layers because some of the transmission parameters it decides are physical layer pa-

rameters. All the transmission parameters are decided by the distributed arbitrator after taking into account the inputs from all the monitors, collision avoidance function and collision resolution function. The two collision related functions are needed as part of the distributed scheduler because collisions are likely to happen when the distributed arbitrator lacks a perfect global information when making transmission decision. While the distributed arbitrator works on a packet-by-packet basis, collision resolution and collision avoidance may or may not work on a packet time scale. As an example of collision avoidance, the CSMA/CA senses for the carrier and reserves the medium using RTS/CTS exchange for each packet. For the same purpose, TDMA uses a deterministic time slot allocation which is performed only once for many packets.

Up to this point, we have described the mechanisms and monitors together with their interactions as illustrated in Fig.3.1. We understand that the figure is not perfect because it does not show all the existing interactions. For example, the route quality in the route monitor is related to the link quality in the channel monitor but this is not shown in the figure. We argue this is to avoid overcrowding the figure while keeping it conceptually correct. The key concept brought up by the framework is summarized as follows: In providing end-to-end QoS in a wireless multi-hop ad hoc network, we need the four mechanisms that are provided with feedback and dynamics by three monitors. These mechanisms and monitors operate across different protocol layers and time scales, and a change in any of the components will directly or indirectly affect the others. For the same purpose to avoid overcrowding, the interactions between the four mechanisms are only shown indirectly through the monitors. For example, the admission control will affect the distributed scheduler by affecting actual QoS measured in the QoS monitor.

3.4 A Realization Scheme: PDMED

In this section, we present a realization of the proposed framework (see Fig.3.1), PDMED, to provide an accurate end-to-end proportional QoS differentiation across multiple hops in a wireless ad hoc network. In PDMED, we have made a few assumptions so that we can focus on the problem of providing an accurate end-to-end proportional differentiation while leaving the other issues such as mobility of nodes, channel errors, re-routing and dynamic admission decision to future research.

3.4.1 Assumptions

We assume that all the traffic flows are self-disciplined such that no traffic policing is required. We further assume that all the nodes are not mobile and have a deterministic route quality so that the static shortest path routing protocol can be adopted. We also assume the use of CSMA/CA MAC protocol. This implies the collision avoidance function consists of RTS/CTS exchange and carrier sensing. Also, the collision resolution function is based on the paradigm that each flow has its own contention window size. Thus, collisions can be resolved by dynamically adjusting the contention window size based on which the back-off duration of a flow is determined. Let W_i be the contention window size of a flow i. Then, the back-off duration of a flow i, Δ_i in terms of number of discrete intervals is decided as follows:

$$\Delta_i = U[0, W_i - 1] \tag{3.1}$$

where $U[x, y]$ is a function that generates random integer numbers within the range $[x, y]$. In (3.1), W_i is adjusted depending on the number of retransmission, m, the current flow i's packet has experienced such that $W_i = 2^m \times W_{\min}$, where $W_{\min}$ is the minimum contention window size of all flows. While W_i increases with the number of retransmissions, it is upper bounded by $W_{\max}$. The adoption of CSMA/CA also means

that the centralized scheduler is implicit. Specifically, with CSMA/CA, only the local flow that has finished first counting down its back-off duration can contend for medium access with the other flows from neighboring nodes.

As a result of the few assumptions given above, the task of providing an accurate end-to-end proportional differentiation falls mainly on a distributed scheduler instead of the other three mechanisms. Thus, we will thereafter focus on designing the distributed scheduler and specifying how the QoS monitor, route monitor and channel monitor should support the scheduler.

3.4.2 Distributed Scheduler and QoS Monitors

In designing the distributed scheduler, we let the QoS be defined in terms of average end-to-end packet delay. Thus, target end-to-end QoS of the QoS monitor to achieve proportional differentiation in Fig.3.1 can be written as follows:

$$\frac{d_i(t)}{\phi_i} = \frac{d_j(t)}{\phi_j}; \qquad \forall i, j, t \tag{3.2}$$

where ϕ_i has been defined earlier in (2.1) and $d_i(t)$ is the actual average end-to-end packet delay for flow i at time t. In practice, $d_i(t)$ must be measured at the destination node of flow i. From the expression above, the target QoS can be interpreted as achieving among all flows an equality in their normalized end-to-end packet delays and the deviation of a flow i from the target QoS at time t can be quantified by $\beta_i(t)$ as follows:

$$\beta_i(t) = \max_{\forall j/i} \left\{ \frac{d_j(t)}{\phi_j} \right\} - \frac{d_i(t)}{\phi_i} \tag{3.3}$$

From the equation, $\beta_i(t)$ is a positive real number where the smaller value means that it is closer to the QoS target, i.e., $\beta_i(t) = 0$. Thus, $\beta_i(t)$ is also used as the measurement for the actual QoS of flow i at time t.

In order to make $\beta_i(t)$ as close as possible to its target value 0, we propose to dynamically adjust the back-off duration of a flow based on its instantaneous deviation from the equality such that a flow with a relatively smaller $\beta_i(t)$ is given a shorter back-off duration to reduce its end-to-end packet delay. On the other hand, a flow with a relatively larger $\beta_i(t)$ is given a longer back-off duration to give way to transmissions from other flows with a smaller $\beta_i(t)$. However, there is no intuitive best known method to perform the adjustment because of the following two problems: (a) The average end-to-end packet delay, $d_i(t)$ that is measured at the destination node is not readily available to the intermediate nodes and source node of the flow, and (b) The normalized end-to-end packet delay of a flow is only known to the flow itself but the computation of $\beta_i(t)$ requires the normalized delays of other contending flows.

Solving the two problems are the functions of the QoS monitor and channel monitor (refer to Fig.3.1), respectively. In the QoS monitor, a backward propagation scheme is proposed so that $d_i(t)/\phi_i$ computed at the destination node will be known by the flow's intermediate and source nodes. According to the backward propagation scheme, when a packet arrives at a flow i's destination node at time t, its average end-to-end delay is updated as follows:

$$d_i(t) = \frac{\tau_i(t) + (n(t) - 1) \times d_i(t')}{n(t)} \tag{3.4}$$

where $\tau_i(t)$ is the end-to-end delay of the packet arrives at time t, $n(t)$ is the total number of packets including the newly arrived one up to time t, and $d_i(t')$ is the previous average packet delay. Through the updating process, the destination node always has the latest value of normalized average end-to-end packet delay, i.e., $d_i(t)/\phi_i$. The latest value together with its respective flow identity will be piggy-backed onto the MAC ACK frames that are transmitted in response to each successfully received MAC DATA frame of the flow. At the intermediate nodes, the piggy-backed information

will be extracted from the received MAC ACK frames and stored locally before being similarly piggy-backed onto the upcoming MAC ACK frames of the flow. As such, the actual normalized end-to-end packet delay of each flow can be propagated from the destination node to the source node. We notice that there will be a time lag between the computation of an instantaneous normalized average end-to-end delay and its arrival at the intermediate and source nodes. In practice, the extend of the time lag depends on the number of hops and its impact on the QoS target will be extensively studied through simulation in the next section.

In the channel monitor, a sniffer is proposed to read all the transmitted MAC ACK frames within a broadcast region. With the sniffer, each node can maintain a table containing the identities of all neighboring flows and their respective latest normalized average end-to-end delays. The table is updated each time a MAC ACK frame is received. With the up-to-date table, $\beta_{i,k}(t)$, i.e., the value of $\beta_i(t)$ (refer to (3.3)) at the k-th hop of flow i can be computed as follows:

$$\beta_{i,k}(t) = \max_{\forall j \in \mathcal{I}_{i,k}/i} \left\{ \frac{d_j(t)}{\phi_j} \right\} - \frac{d_i(t)}{\phi_i} \tag{3.5}$$

where $\mathcal{I}_{i,k}$ is the set of flow i's neighboring flows at its k-th hop. Based on the computed $\beta_{i,k}(t)$, flow i can rank itself among all its neighboring flows. Specifically, the flow will be given the rank l if its $\beta_{i,k}(t)$ is the l-th highest among all the neighboring flows.

Let $r_{i,k}$ be the rank of flow i at its k-th hop when it has a packet to transmit there but sense a busy channel. In case no ranking can be performed, the default value for $r_{i,k}$ is unity. Also, let $W_{i,k} = 2^{m_{i,k}} \times W_{\min}$ be the flow's contention window size at its k-th hop when the packet is making the $m_{i,k}$-th retransmission attempting and $m_{i,k} = 0$ for a fresh packet. Then, instead of the using the original CSMA/CA method in (3.1), the

distributed scheduler will decide the flow's back-off duration, $\Delta_{i,k}$ as follows:

$$\Delta_{i,k} = \begin{cases} U[0, W_{\min} - 1] + I_{r_{i,k} \geq 2} \times \gamma_{i,k} \times W_{\min} & \text{if} \quad m_{i,k} = 0 \\ U[0, \frac{W_{i,k}-1}{h_i}] + W_{i,k} \times (\frac{h_i - k}{h_i} + r_{i,k} - 1) & \text{otherwise,} \end{cases} \tag{3.6}$$

where h_i is the total number of hops for flow i and it is provided to the distributed scheduler by the route monitor in Fig.3.1. In (3.6), the term I_A is an indicator function defined as follows:

$$I_A = \begin{cases} 1 & \text{if A is true} \\ 0 & \text{otherwise,} \end{cases} \tag{3.7}$$

where A represents any condition. And $\gamma_{i,k}$ is a dynamic control parameter for flow i at its k-th hop. The control parameter has an initial value of unity and it is dynamically adjusted only for a fresh packet at time t based on the actual normalized average end-to-end delay as follows:

$$\gamma_{i,k} = \begin{cases} \gamma'_{i,k}(t') + 1 & \text{if} \quad 0 < \beta_{i,k}(t') < \beta_{i,k}(t) \\ \gamma'_{i,k}(t') - 1 & \text{if} \quad \beta_{i,k}(t) = 0 \quad \text{and} \quad \gamma_{i,k}(t) > 1 \\ \gamma'_{i,k}(t') & \text{otherwise,} \end{cases} \tag{3.8}$$

where $\beta_{i,k}(t')$ and $\gamma'_{i,k}$ are the previous values of $\beta_{i,k}(t)$ and $\gamma_{i,k}$, respectively.

Comparing (3.6) and (3.1), we notice that the proposed distributed scheduler gives priority to a flow that is experiencing excessive normalized average end-to-end delay by allowing a smaller back-off duration. In order to ensure a high responsiveness of the proposed mechanism, $\gamma_{i,k}$ provides an additional degree of freedom when ranking and prioritization alone are not sufficient to quickly bring down a high normalized delay. Also, the proposed method gives priority to a retransmitted packet compared to a fresh packet. This is to avoid the situation where multiple packets from a same flow are contending with each other arbitrarily. Among all the retransmitted packets, based on the heuristic disclosed in [33], the packet that is closer to the destination node will

be given the priority to transmit so that the overall end-to-end delay can be reduced.

In PDMED, the message overhead is only the QoS performance value in QoS monitor at the destination which is fed back to the source. The value is a float number that only requires 2 bytes in ACK frame. No other message and separate frame are needed.

3.5 Performance Evaluation

We have evaluated the proposed PDMED through random event simulations using OPNET [40]. For the purpose of simulation, the general static network topology as illustrated in Fig.3.2 is used first. In the network, there are only two flows, namely Flow 1 ($S1 \rightarrow D1$) and Flow 2 ($S2 \rightarrow D2$). From the figure, Flow 1 and Flow 2 have 3 and 2 hops, respectively. For the flows, their differentiation parameter are denoted by ϕ_1 and ϕ_2, respectively.

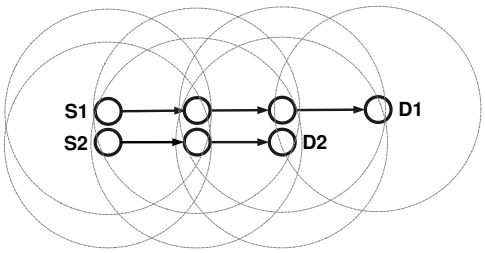

Figure 3.2: Topology of simulation scenario with different hops

In the simulations, traffic for each flow is generated using a Poisson arrival process with a fixed packet size, L_m and a packet arrival rate, λ. Hence, the packet inter-arrival time is exponentially distributed with mean λ^{-1}. Hereafter, L_m is fixed at 500 bytes unless specified otherwise. In the evaluation, the raw bit rate of communication channel is 1 Mbps. Also, refer to (3.1), W_{min} and W_{max} for the proposed realization are fixed at 16 and 1024 time slots, respectively. Here, the duration of each time slot, $T_{slot} = 50\mu s$.

In addition, the delay of a packet is the time elapsed since the packet's arrival at the MAC layer of its source node until the packet's subsequent arrival at the MAC layer of its destination node. These packets from their respective traffic sources are queued above but not in the MAC layer to avoid distortion in packet delay at high traffic rate, λ^{-1} when the delays of all flows increase exponentially making any difference in their values not noticeable. Different ϕ_2/ϕ_1 ratios are achieved by fixing ϕ_1 at 1 while varying ϕ_2.

3.5.1 Backward Propagation Scheme

First of all, we perform simulations to study the usefulness of the backward propagation scheme adopted by the QoS monitor to inform the nodes of a flow's instantaneous normalized end-to-end delay. Recall that the backward propagation is achieved by piggy-backing the latest delay value onto the MAC ACK frames. We disable the piggy-backing in some simulations and compare the results with those of the normal PDMED. The comparison is depicted in Fig.3.3 which shows the performance in terms of average end-to-end packet delay. The results show that PDMED can indeed provide a proportional differentiation in packet delay despite the flows are going through different numbers of hops. When there is an increase in ϕ_2/ϕ_1, the proportional differentiation is indicated by the more rapid increase in Flow 2's end-to-end delay compared to that of Flow 1 although Flow 2 has fewer hops. Also, Flow 2's delay increases faster than that of Flow 1 with respect to a decrease in λ^{-1}.

Fig.3.3 has confirmed the importance of the backward propagation scheme because, without it, the difference between the two flow's delays is not obvious at various ϕ_2/ϕ_1 ratios. This is further verified in Fig.3.4 where the difference between the two flow's normalized average end-to-end packet delay is plotted. Ideally, the difference should

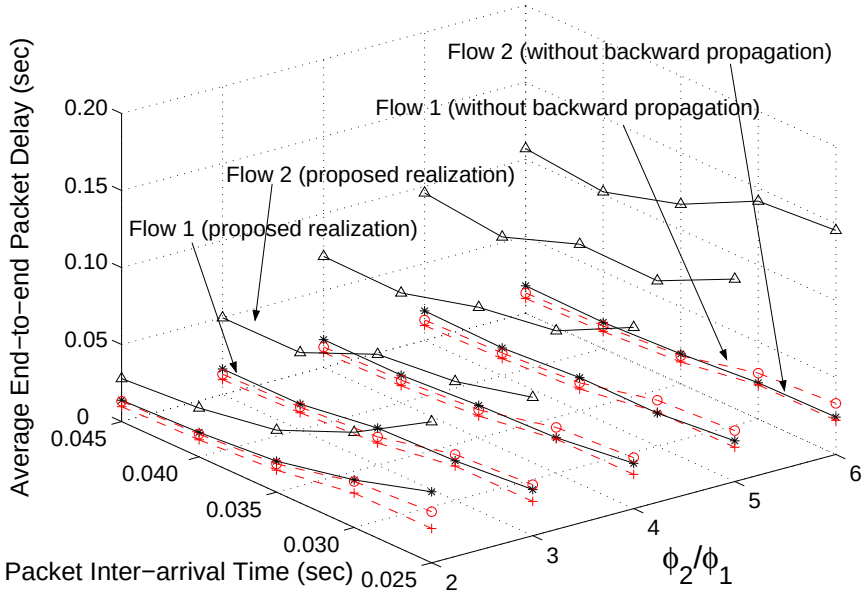

Figure 3.3: Average end-to-end packet delay with/without backward propagation scheme

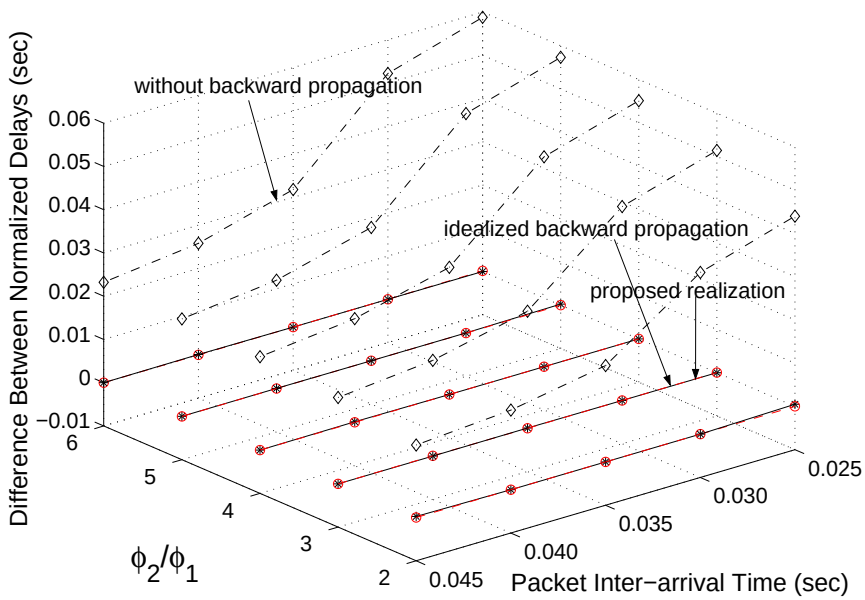

Figure 3.4: Difference between the normalized end-to-end packet delay of two flows with/without backward propagation scheme

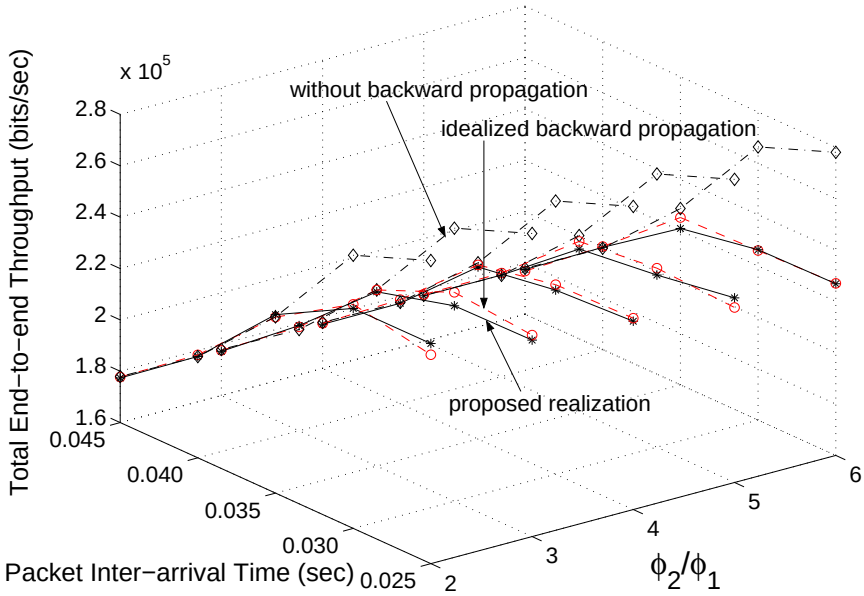

Figure 3.5: Total end-to-end throughput of two flows with/without backward propagation scheme

be zero because, as stated in (3.2), the performance goal is to achieve equality in the normalized delays. From Fig.3.4, PDMED can indeed approximate the performance goal regardless of the traffic rate and ϕ_2/ϕ_1 ratio. On the other hand, the performance goal is not achievable when there is no backward propagation. This happens because, in the absence of the backward propagation, the intermediate nodes do not know the actual end-to-end delay and thus, cannot adjust its back-off duration appropriately to meet the performance goal.

In the evaluation above, the backward propagation scheme is disabled by simply not piggy-backing the computed normalized delay on ACK frames. While this leads to a failure in accurate proportional differentiation, there is a noticeable gain in total end-to-end throughput of the two flows as depicted in Fig.3.5. This is because, without the instantaneous normalized delay, an intermediate node cannot correctly compute $\beta_{i,k}(t)$ according to (3.5) and consequently, will not perform the ranking mechanism and adjust $\gamma_{i,k}$ according to (3.8). Without the ranking and adjustment, $r_{i,k}$ and $\gamma_{i,k}$

stay at their default values of unity. Thus, the back-off duration will always be selected from a range upper bounded by $W_{min} - 1$ compared to a potentially much larger range adjusted by ranking and $\gamma_{i,k}$ according to (3.6). The smaller back-off duration is the cause of the better end-to-end throughput when there is no back-off propagation. In the presence of backward propagation, we treat the reduction in throughput as the cost to pay for the accurate proportional differentiation.

The ranking in PDMED may not always be based on the latest instantaneous normalized delay because the backward propagation scheme takes time to distribute the delay across multiple hops after it is computed at the destination node. Specifically, there is always a time lag before the latest normalized delay is available at an intermediate node. Fortunately, this time lag has no significant impact in achieving an accurate proportional differentiation in average end-to-end delay as illustrated in Fig.3.4. In the figure, there is no obvious difference in performance when PDMED is equipped with an idealized backward propagation scheme. Compared to the original scheme, the idealized scheme does not require piggy-backing of the latest delay on ACK frames. Instead, the simulation program makes the delay known to all the intermediate nodes as soon as it is computed. Without piggy-backing, the idealized propagation scheme consumes less bandwidth. However, as shown in Fig.3.5, there is no obvious throughput difference between the original and idealized back propagation schemes. This implies the backward propagation scheme is efficient as it introduces only very small overhead.

3.5.2 γ Adjustment

Thus far, we have shown the importance and effectiveness of the backward propagation scheme in PDMED. In short, the backward propagation is needed so that intermediate nodes can obtain the instantaneous normalized delay for ranking and $\gamma_{i,k}$ adjustment

to achieve an accurate proportional differentiation. Next, we want to show that the ranking itself, without $\gamma_{i,k}$ adjustment is not sufficient. For this purpose, we have repeated the simulations after disabling the adjustment algorithm in (3.8). Fig.3.6 shows the difference between the two flows' normalized average end-to-end packet delay. Compared to the normal PDMED, the difference is much larger which indicates a less accurate proportional differentiation when there is no $\gamma_{i,k}$ adjustment. This means the ranking mechanism alone is not enough in the channel monitor.

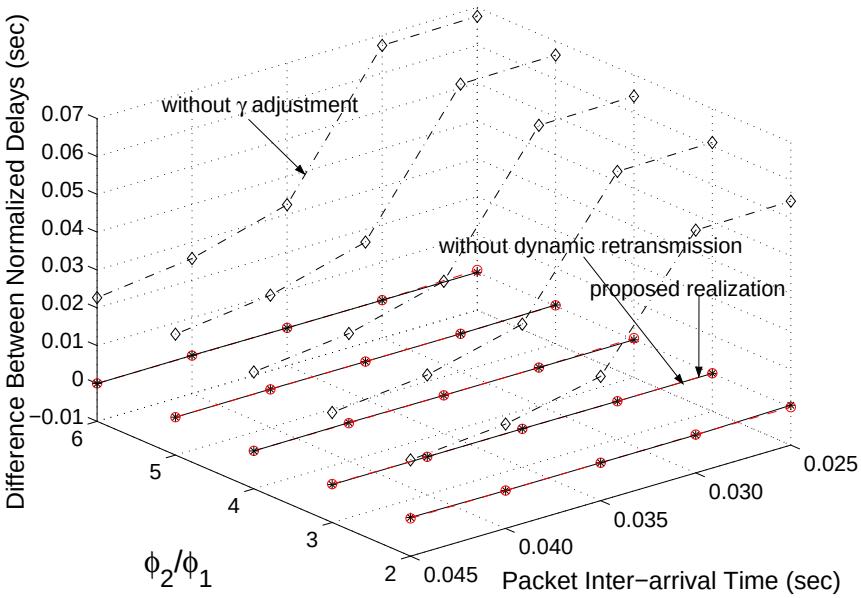

Figure 3.6: Difference between the normalized end-to-end packet delay of two flows with/without γ adjustment and dynamic retransmission

Although the absence of $\gamma_{i,k}$ adjustment cannot produce an accurate proportional differentiation, it results in higher total end-to-end throughput as illustrated in Fig.3.7. Refer to (3.6), this is because the back-off duration tends to be smaller when $\gamma_{i,k}$ is not dynamically adjusted but fixed at its initial value of unity. The better throughput without $\gamma_{i,k}$ adjustment also leads to a lower end-to-end packet delay as illustrated in Fig.3.8. Despite a lower delay, when there is no $\gamma_{i,k}$ adjustment, the difference in delay does not follow the ϕ_2/ϕ_1 ratio and thus does not constitute an accurate proportional

differentiation.

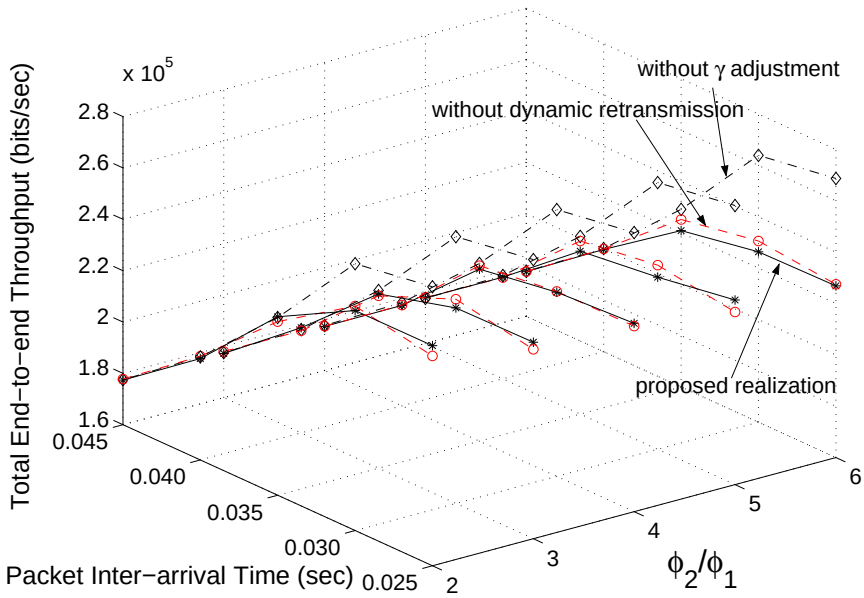

Figure 3.7: Total end-to-end throughput of two flows with/without γ adjustment and dynamic retransmission

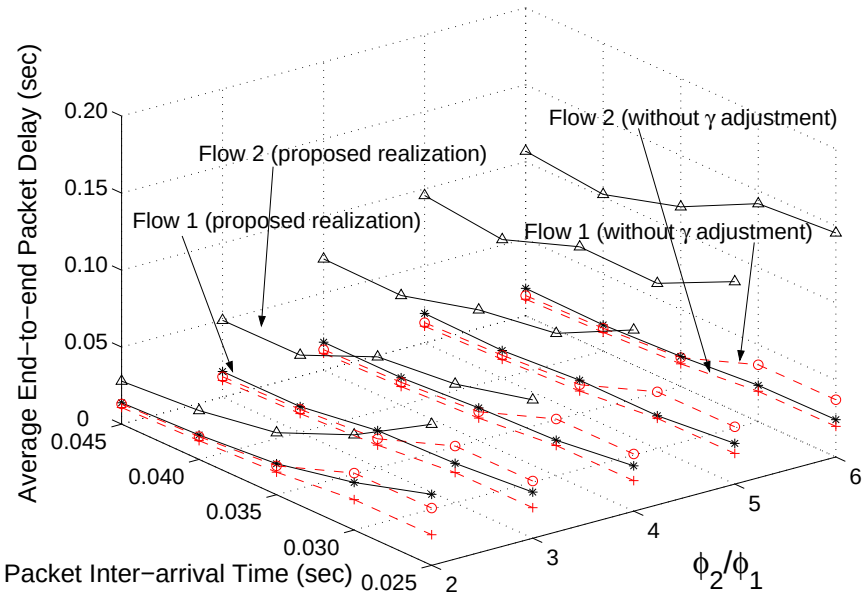

Figure 3.8: Average end-to-end packet delay with/without γ adjustment

3.5.3 Retransmission Scheme

In Fig.3.9 we show the impact of the dynamic retransmission scheme in PDMED. As given in (3.6), a retransmission is indicated by $m_{i,k} > 0$ and the dynamic retransmission scheme gives higher priority to transmissions from a node closer to a flow's destination node. As such, PDMED can deliver a smaller end-to-end delay compared to the case without the dynamic retransmission scheme. The simulations without the retransmission scheme have been performed by simply selecting the back-off duration, i.e., $\Delta_{i,k}$ in (3.6) from the range $[0, W_{i,k} - 1]$ when $m_{i,k} \neq 0$. While the dynamic retransmission scheme in PDMED is capable of reducing end-to-end delay, it does not compromise the accuracy of proportional differentiation and total throughput as illustrated in Fig.3.6 and Fig.3.7, respectively.

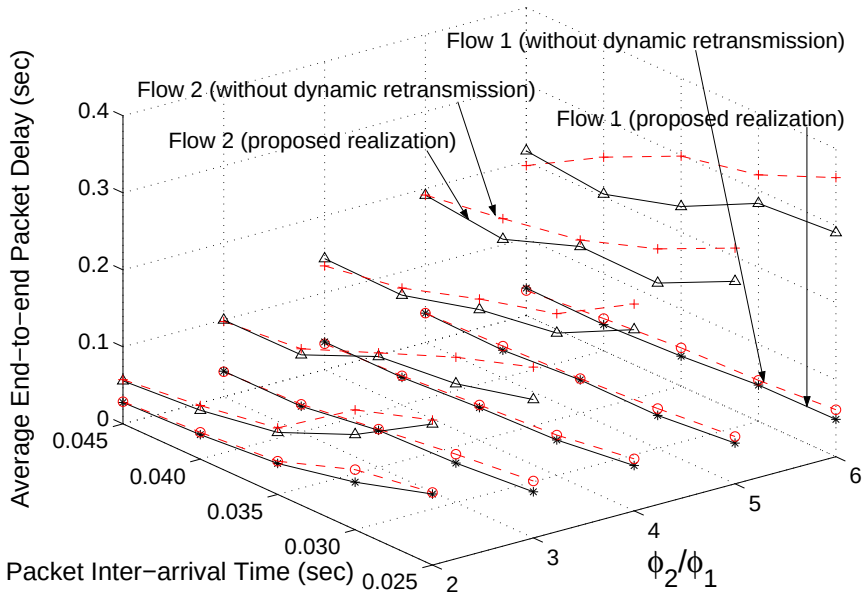

Figure 3.9: Average end-to-end packet delay with/without dynamic retransmission

3.5.4 Video Traffics and Benchmark to IEEE 802.11e

After verifying the importance of various components in PDMED, we next study its performance under different traffic conditions. For this purpose, we replace the Poisson traffic source with video traces from [42]. Specifically, we use video traces coded by H.263 at 265 Kbps. Each of the coded video frames can be few thousand bytes and thus, potentially larger than the supported maximum MAC DATA frame payload size, i.e. 2000 bytes. When this occurs, the oversized video frame is fragmented into multiple smaller frames of 2000 bytes with the final frame contains the residual bytes. The calculated average end-to-end delay of a packet is the time between the generation of the packet to its arrival at the destination.

To begin with, we use the video trace from movie Jurassic Park. Although both Flow 1 and Flow 2 use the same video trace, they have different time offsets. The offsets for Flow 1 and Flow 2 are 0 and 300 seconds, respectively. This means Flow 2 starts playing the movie from its 300-th second. Fig.3.10 shows the average end-to-end packet delay for different ratios of ϕ_2/ϕ_1. From the figure, the average packet delay for Flow 1 equals that of Flow 2 when $\phi_2/\phi_1 = 1$. Similarly, when $\phi_2/\phi_1 = 2$, the average delay of Flow 2 is double compared to that of Flow 1. This is a clear indication of an accurate proportional differentiation when the multi-hop ad hoc network is loaded with the actual video trace from movie. As depicted in Fig.3.10, this accuracy in proportional differentiation is consistent when the evaluation is repeated using different video traces from other movies, namely Silence of the Lams and Star War.

Next, we benchmark PDMED against IEEE 802.11e which is designed to provide QoS differentiation in a wireless ad hoc network. Different from PDMED, IEEE 802.11e achieves its goal by selecting an appropriate traffic class and setting different mini-

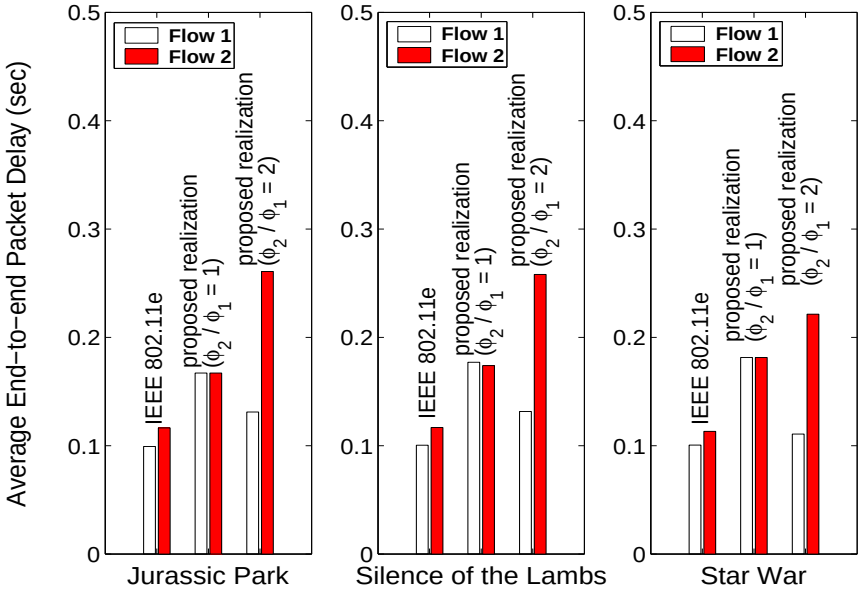

Figure 3.10: Average end-to-end packet delay with different video traces

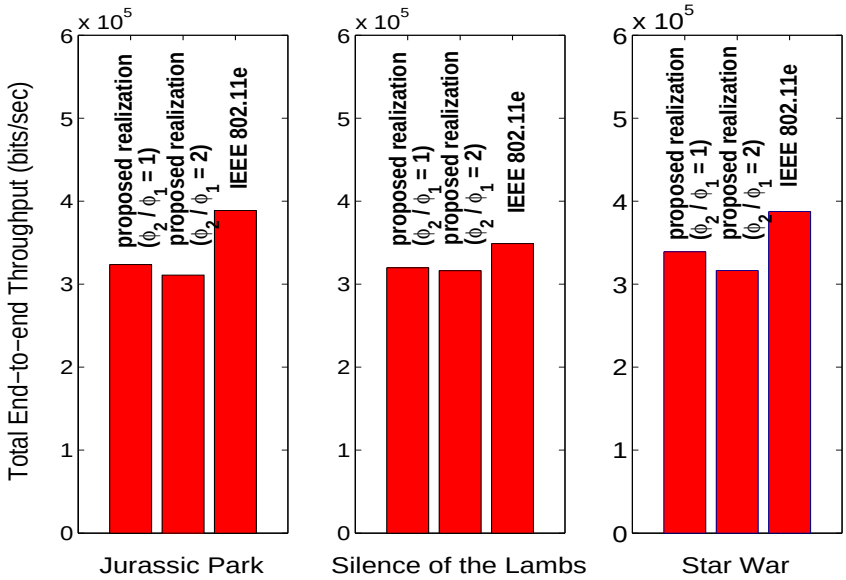

Figure 3.11: Total end-to-end throughput of two flows with different video traces

mum and maximum contention window sizes, which are denoted by W_{min} and W_{max} in (3.1) for different flows within the selected traffic class. For this benchmark, we let both flows be from the same traffic class because PDMED does not have the concept of traffic classification and achieve its performance goal only by adjusting contention window size of a flow. Unfortunately, there is no standardized method in IEEE 802.11e on how to set the contention window sizes to achieve its performance goal. Recall the finding in [13] which suggests that the one-hop average delay of an IEEE 802.11 flow is proportional to its minimum contention window size. Hence, we fixed the maximum contention window size at 1024 time slots while setting the minimum contention window sizes for Flow 1 and Flow 2 to 16 and 32 time slots, respectively. This is for the wish to make Flow 2's average end-to-end packet delay two times of that of Flow 1's.

For the evaluation described above, Fig.3.10 shows that IEEE 802.11e is not capable of providing an accurate proportional differentiation in end-to-end packet delay for all the three movies. In the figure, despite failure in accurate proportional differentiation, IEEE 802.11e gives a lower average end-to-end delay. This is because IEEE 802.11e tends to have a smaller back-off duration compared to PDMED, especially when $\gamma_{i,k}$ grows to a bigger value to provide accurate differentiation. For the same reason, Fig.3.11 shows that PDMED yields a lower throughput compared to IEEE 802.11e. The smaller throughput and higher delay are the cost incurred by PDMED in achieving the accurate proportional differentiation.

3.5.5 Video Traffics in Mobility Scenario

Above video traffics evaluations are conducted based on static node positions and network topology although different flows have different hops in their transmission paths. Now, we continue to evaluate PDMED with video traffics in mobility scenario via sim-

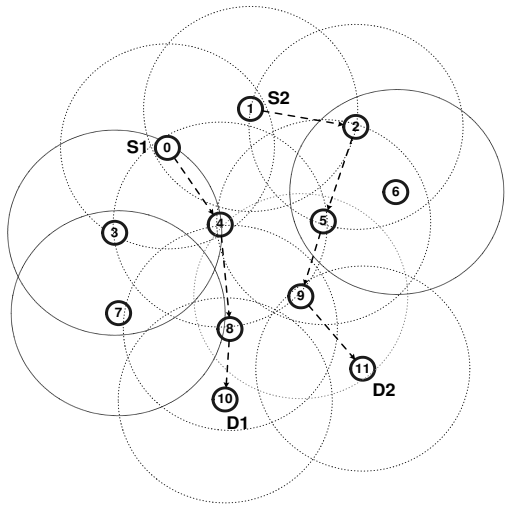

Figure 3.12: An example of network topology with mobile nodes

ulations.

When building a mobility scenario, a routing protocol support is necessary. AODV routing protocol which is widely adopted in evaluations of ad hoc network is used in our simulations. We define nodes moving within a 2000×2000 m^2 area and put 12 nodes, which are denoted by $0 - 11$, in this area . Nodes are distributed arbitrarily in the area initially. Fig. 3.12 shows an example of this network topology.

All of nodes move according to random waypoint model with speeds defined by a uniform distribution function, $U[0, y]$ that refers to a uniform distribution between 0 and y. This time, we only use the video traces from movie Jurassic Park, which is coded by H.263 at 265 Kbps. The same as before, the frame which is larger than 2000 bytes, maximum DATA frame payload size that MAC layer supports, is fragmented into several frames of 2000 bytes and the final frame containing the residual bytes. Two flows, denoted as $F1$ and $F2$, are deployed in such a network. We define that $F1$ initiated by node 0 destines at node 10 and $F2$ initiated by node 1 destines at node 11. $F1$ and $F2$ are both video traffics of Jurassic Park, but with different offsets of start time, 0 and 300 seconds respectively. The differentiation ratio, ϕ_2/ϕ_1, is set as $2 : 1$ between

$F1$ and $F2$. We choose five speed scenarios for evaluation, $U[0, 20]$, $U[0, 40]$, $U[0, 60]$, $U[0, 80]$ and $U[0, 100]$ (m/s).

In Fig.3.13, good differentiation ratios between the average end-to-end delay of two flows are exhibited in all speed scenarios. This shows that PDMED is still able to achieve good proportional differentiation in end-to-end QoS between flows even if nodes move at randomly with various speeds. Although the transmission hops of every flow change randomly due to random movement of nodes, PDMED also accurately control the ratios of resource utilization between flows. The accuracy of proportional differentiation is also shown in Fig. 3.14. We also see in Fig. 3.13 that the average end-to-end packet delay becomes larger when the moving speed increases from $U[0, 20]$ (m/s) to $U[0, 40]$ (m/s), and then becomes smaller slowly after the moving speed increases over $U[0, 40]$ (m/s). The reason is that, when moving speeds of nodes are slow, the link between nodes are stable. Thus re-routing seldom happens so that the end-to-end packet delay is low. When speed increases, link break happens more and more. Then the end-to-end packet delay increases due to waiting for re-routing actions. However, when speed keeps increasing, although re-routing may happen more often, it is easier to re-route a path for a flow because nodes are faster to move close to each other. Although re-routing action can be faster to find a new path when nodes move in high speeds, it is impossible to tradeoff the packet delay due to waiting for a new path. Therefore, we see such a trend of the average end-to-end packet delay in Fig.3.13.

Actually, besides the moving speed of nodes, the density of nodes in the network also affects the link stability. If there are less nodes move in a network, it is more difficult in finding a new path. Thus, we also repeat the above simulation in a $3000 \times 3000\ m^2$ area. Because the moving area is increased by 1.5 times, it is obvious that the number of hops of a flow is potentially increased. Thus, the average end-to-end packet delay

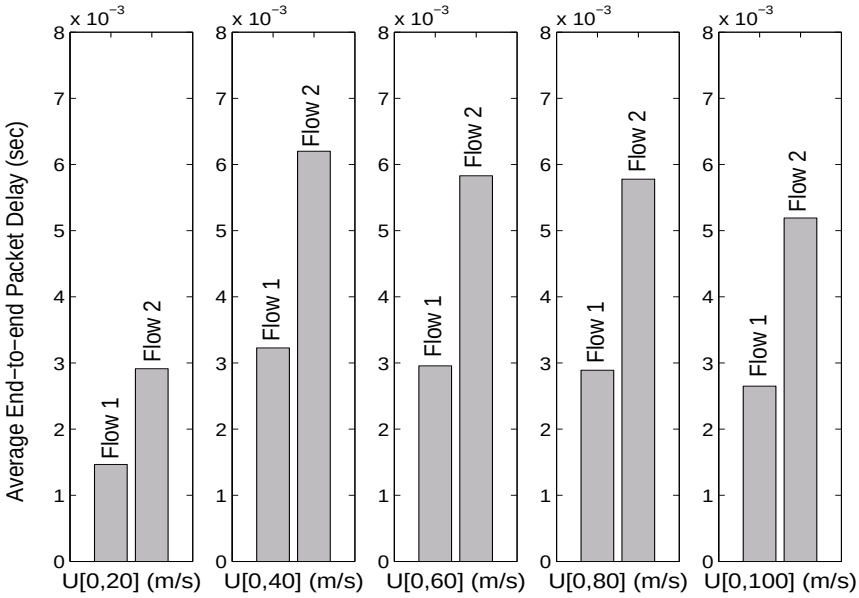

Figure 3.13: Average end-to-end delay by different speed scenarios

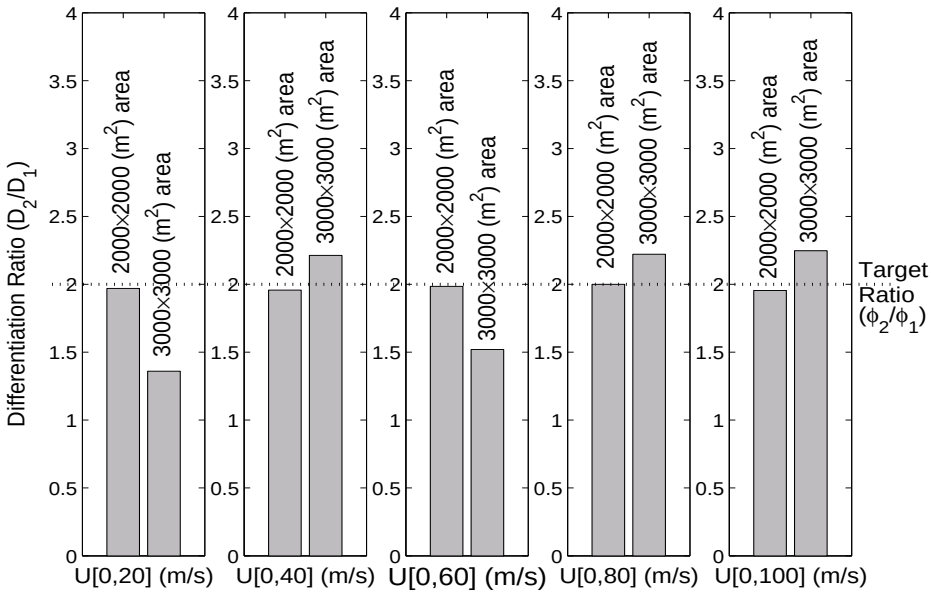

Figure 3.14: Ratios of average end-to-end delay between flows by different speed scenarios

should increase. In following, we focus on comparing the proportional differentiation performance between two scenarios of moving area. In Fig. 3.14, we compare the achieved differentiation ratio, D_2/D_1, between two scenarios. Here, D_2 and D_1 are the average end-to-end packet delay of Flow 2 and Flow 1. Obviously, when the moving area of nodes increases to 3000×3000 m^2, the accuracy of proportional differentiation performance is affected. Although there is still differentiation between two flows, the ratio is far from the target ratio, ϕ_2/ϕ_1. Because lower density of nodes in the network increases the difficulty of finding a new path, the duration of link break is also increased. Thus link break happening can dynamically vary the end-to-end packet delay greatly. The figure shows that PDMED is not capable enough to compensate this variation completely. And this phenomenon also indicates that, the effect of link break on proportional differentiation of PDMED is much larger than the dynamical changing transmission hops. In order to support proportional differentiation in such kind of networks with long time of link break, another mechanism, such as in QoS routing in our framework or a controller on node distribution in network, is needed to co-operate to PDMED. This problem is out of scope of this thesis.

Because the link break definitely reduce the network resources, the total end-to-end throughput of two flows in 3000×3000 m^2 scenario is reduced, compared to 2000×2000 m^2 scenario, as shown in Fig.3.15. From the figure, we also see the trend of total throughput of network with the increasing of nodes' moving speeds. When the moving speeds of nodes are low, the total throughput of network is the highest because the wireless links between nodes are robust. With the increasing of the moving speeds, the total throughput of network is reduced due to more happenings of link breaks. The packets have to wait for establishing a new path. When the moving speed keeps increasing, the total throughput of network becomes high again because of faster es-

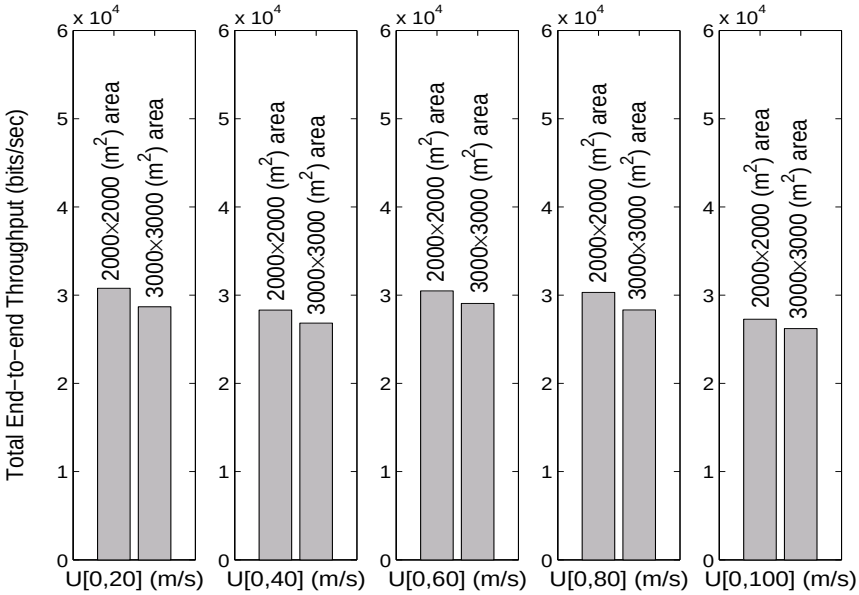

Figure 3.15: Total throughput by different speed scenarios

tablishment of a new path. However, after then, with the continuous increasing of the moving speed, the total throughput decreases. The reason is, frequently changes of transmission pathes increase happening of packet to wait for re-routing a new path and thus reduces the network resource.

3.6 Conclusions

Noticing the lack of support in providing end-to-end proportional differentiation in a wireless multi-hop ad hoc network, this chapter first presents a generic cross layer framework to do so. The framework suggests that meeting QoS objective requires 4 mechanisms and 3 monitors which operate across different protocol layers and time scales, and a change in any of the components will directly or indirectly affect the others. Given the framework, a specified realization, PDMED, has been presented for proportional differentiation in end-to-end average packet delay. PDMED has been extensively evaluated through random event simulations. The results indicate that an accurate and consistent proportional differentiation which cannot be achieved other-

wise, can now be achieved. Benchmark against IEEE 802.11e using various video traces shows that the accurate proportional differentiation is achieved at a small cost in terms of a higher packet delay and a lower throughput. The evaluation results in mobility scenarios show that PDMED still achieve a good proportional differentiation in mobility scenario when the node density of network is high enough. And its performance may be degraded by low node density in network.

Chapter 4

An Improvement Scheme in Mobility and Time-varying Channel Scenario

4.1 Introduction

In chapter 3, although we have achieved the goal of proportional differentiation on average end-to-end delay in a wireless multi-hop ad hoc network, in which nodes move according to random waypoint model. However, obviously mobility of nodes and time-varying channel quality are two factors that greatly reduce the available network resource and affect the performance of flows in wireless multi-hop ad hoc networks. Time-varying wireless channel quality can affect signal-to-noise ratio of a packet transmission and whether it can be transmitted successfully. Mobility of nodes can lead to link breakage, variation of hops of a flow path and variation of the signal strength of a packet transmission. In the networks based on broadcasting transmission pattern of wireless mediums, mobility of nodes also instantaneously vary the interferences because

some other nodes may transmit packets simultaneously.

Recall that PDMED dynamically adjusts the scheduling parameters based on the instantaneous end-to-end QoS performances of all flows in networks in order to achieve the proportional differentiation between flows. The variation of the end-to-end performance of one flow will bring variation on the end-to-end performances of its neighboring flows and even all other flows in the network. Thus, when mobility of nodes and time-varying channel affect the instantaneous end-to-end QoS value of one flow, the end-to-end QoS values of other flows are also affected soon after. And, the more variations of wireless channel happen due to mobility and time-varying channel, the larger deviation of the instantaneous proportional differentiation ratio among flows from the target ratio is generated. In PDMED, in order to compensate this effect and achieve proportional differentiation accurately, the performance of flows, such as delay or throughput, has been traded off. An support for PDMED that handles variations on packet transmissions due to mobility of nodes and time-varying channel in physical layer is quite necessary for increasing utilization of network resource, robustness and accuracy of PDMED in the environment with mobile nodes and time-varying channel quality.

In chapter 2, we have investigated the existing methodologies to handle mobility of nodes and time-varying channel quality. Among them, some track and predict mobility of nodes ([26], [27], [28]). Others capture time-varying channel quality based on cellular wireless networks ([29], [30], [31]). Otherwise, some work gives an estimation of the upper bound of signal-to-noise ratio in the point of view of a whole ad hoc network [32]. No one is able to capture instantaneous effects of mobility of nodes and time-varying channel on packet transmissions in wireless multi-hop ad hoc networks based on CSMA/CA. Thus they are unable to help improving the performance of PDMED

in the environment with mobility of nodes and time-varying wireless channel.

In this chapter, we will intensively study the effects on packet transmissions generated mainly by movements of nodes in wireless ad hoc networks because mobility generates more variation factors which affect packet transmissions, such as signal strength, number of interference nodes and interference strength, hops of transmission path, duration of link break, etc., compared to time-varying characteristics of wireless medium environment. After that, utilizing the result of our study, we will propose an improvement of PDMED, PDMED+.

Our contributions in this chapter are: 1) we discovered that, based on random waypoint mobility model, the SINR value we defined for a packet transmission exhibits self-similar characteristic. 2) Based on the self-similarity of SINR, we suggested a forecasting method to predict the value of SINR series in one-step ahead. Then we proposed an improvement scheme of PDMED, PDMED+, to improve network throughput while providing proportional differentiation with the support of predictable SINR values in physical layer in wireless multi-hop ad hoc networks.

In the remainder of this chapter, we will first present our study on SINR in wireless multi-hop ad hoc network in which nodes move under random waypoint model. Next, we will introduce a way to predict the value of SINR series and analyze the accuracy of the predicted SINR series. Finally, we will focus on an improvement of PDMED, PDMED+, and evaluate its performance via simulations.

4.2 Self-similarity of SINR in Ad Hoc Networks

In order to capture the instantaneous effects of mobility on packet transmission in wireless link, we studied how the movement of nodes changes the SINR of a packet

received at the receivers because SINR is the parameter directly reflecting whether a packet is transmitted successfully after being transmitted through wireless channel. We proposed a simple scenario and studied SINR via simulations.

4.2.1 Network Model and Assumptions

We choose the widely adopted random waypoint mobility model to define the movement of nodes as it appears to create realistic mobility patterns for the way people might move [34]. The same network scenario is adopted here as in Fig. 3.12 in the last chapter. There are 12 nodes whose movement is limited in an area of $3000 \times 3000m^2$. We also denote all the nodes by numbers from $0 - 11$, as node ID.

Because in random waypoint model the nodes move in a straight line from a current site to the next site, no obstacle is considered between two sites. So we choose free space propagation model [35] to define the received signal strength as (4.1), which assumes that transmitter and receiver have a clear, unobstructed line-of-sight path.

$$P_r(d) = \frac{P_t G_t G_r \lambda^2}{(4\pi)^2 d^2 L} \tag{4.1}$$

where P_r is the received power which is a function of the T-R (transmitter to receiver) separation, P_t is the transmitted power. G_t and G_r are the transmitter antenna gain and the receiver antenna gain, d is the T-R separation distance in meters, L is the system loss factor not related to propagation ($L \geq 1$), and λ is the wavelength in meters. In order to simplify our model to focus on mobility and wireless channel characteristic, we set all of G_t, G_r and L as 1.

Because of the shared wireless channel in ad hoc networks, the interference for a transmitting packet is related to the traffic pattern and MAC protocols. With the purpose to utilize the channel characteristic to improve medium access of packets, we cannot

study SINR using the real interference calculated according to the traffic generation and medium access patterns. In order to eliminate the relation between interference and medium access of packets, we proposed an estimation model for SINR definition.

Based on the definition of received signal strength in (4.1), we define SINR as the ratio of the received signal strength of a target packet transmission divided by the sum of received signal strength of the other packet transmissions simultaneously (i.e. interference) including background noise, at the point of view from a receiver. However, we assume that all the nodes, whose locations are out of the broadcasting coverage of the transmitter of the target transmission, transmit packets simultaneously so that there is no relation between interference and medium access of packet transmissions. In this way, the calculated interference may be larger than the interference that happens in reality. Thinking of a threshold of SINR which is used to decide whether a packet transmission is successful, we can adjust the threshold to make the decision on a packet transmission approximately consistent to the reality. Thus, this definition of SINR is still meaningful for collecting information about packet transmission in wireless channel. The following formula shows the definition of SINR of a transmission from node i to node j:

$$SINR(i,j) = \frac{P_r(i,j)}{\sum\limits_{k \notin B_t, B_r} P_r(k,j) + N_b} \tag{4.2}$$

where $P_r(i,j)$ is the received power of a packet from node i to node j. k denote the nodes that are out of radio coverage of transmitter of target transmission. B_t is the set of the nodes located in the radio coverage of receiver node of a target transmission. B_r is the set of nodes located in the radio coverage of transmitter node of a target transmission. N_b is background noise.

4.2.2 Simulation Results and Analysis

With the SINR definition, we conducted a simulation experiment to study the characteristic of SINR due to mobility of nodes. We used the example network scenario in Fig.3.12, 12 nodes in the area of $3000 \times 3000(m^2)$. The nodes move in random waypoint model with random speeds defined by uniform distributions. We chose 5 speed scenarios for our experiment, $U[0, 20]$, $U[0, 40]$, $U[0, 60]$, $U[0, 80]$ and $U[0, 100](m/s)$ respectively for analysis. Here, $U[x, y]$ represents a uniform distribution between x and y. We recorded the position of every node, and calculated the distance and the SINR between any two nodes with a sampling interval of 0.01 second for a period of 1000 seconds. The SINR value is calculated for a transmission from a transmitter node and a receiver node. Thus, for any two nodes, we collect two sets of SINR series for one acting as a transmitter and the other acting as a receiver, and vice versa.

We used variance-time plot methodology [36] to analyze the data. Specifically, a data series X with a length of N is divided into N/m blocks by a block size, m. And the average value of each block, $\bar{X}_k^m$, and the estimation of variances of data in each block, $\bar{V}_{X_k}^m$, are calculated, $k = 1, 2, ..., N/m$. Using these $\bar{X}_k^m$ and $\bar{V}_{X_k}^m$, we can obtain the variance of the whole data series as following:

$$V_X^m = \frac{1}{N/m} \sum_{k=1}^{N/m} (\bar{V}_{X_k}^m)^2 - (\frac{1}{N/m} \sum_{k=1}^{N/m} \bar{V}_{X_k}^m)^2 \tag{4.3}$$

With the logarithm of the different block size, m, and the logarithm of corresponding V_X^m, we can use least squares line fitting to calculate the estimated slope of the fitting line and the correlation coefficient, r, which is calculated by following formula:

$$r = \frac{\sum_{i=1}^{n} V_X^{m_i} m_i - n\bar{V}_X^m \bar{m}}{\sqrt{\left(\sum_{i=1}^{n} m_i^2 - n\bar{m}^2\right)\left(\sum_{i=1}^{n} (V_X^{m_i})^2 - n(\bar{V}_X^m)^2\right)}} \tag{4.4}$$

where n is the number of different block sizes, m. We denote the block sizes from the smallest to the largest as $m_i = m_1, m_2, ..., m_n$. $\bar{m}$ is the average of m_i. $\bar{V}_X^m$ is the average of $V_X^{m_i}$ for every m_i. r expresses how a perfect linear fit exists betweens the discrete points. In general, a reasonable fit requires, $0.75 \leq |r| \leq 1$.

We showed three numeric results, the slope of the fitting line by log-log correlogram, hurst parameter and correlation coefficient of least square line fitting of any two nodes for every speed scenario of $U[0, 20]$, $U[0, 40]$, $U[0, 60]$, $U[0, 80]$ and $U[0, 100](m/s)$ respectively in Appendix (shown in Table 1, 2, 3, 4, 5). In the tables of Appendix, **n-n** denotes the a pair of nodes (transmitter node to receiver node) by its ID number. β denotes the slop of log-log correlogram (The log of the sample variance against the log of the sample size). **H** denotes the Hurst Parameter that is given by $H = 1 - \beta/2$. **r** is the correlation coefficient for least square line fitting.

From the analysis results, we can see that the SINR series between any two nodes in the network exhibits self-similar because the Hurst parameters calculated are all between 0.5 and 1.0. This means that the SINR series between any two nodes have short or long-range dependency characteristics. Therefore, through signal processing methods, we are able to find out the parameters of the characteristics of the SINR series and forecast the values of SINR ahead. We are also able to predict the value of SINR before transmitting a packet which provides the information of condition of physical layer before putting the packet into physical layer from MAC layer. This discovery serves a good basis for designing an improved scheme later.

4.3 Prediction Method and Estimation of Prediction Error

From the results in previous section, we discovered that SINR between a transmitter node and a receiver node exhibits self-similar characteristic. Thus, it is feasible to forecast the SINR value based on the history data in a SINR series. We use fractionally integrated autoregressive moving average process (F-ARIMA) time-series to model our SINR series . There are a lot of prediction methods based on F-ARIMA process in literatures, such as ([37], [38], [39]). We choose the method in [37] for prediction because of its simplicity.

The steps of this prediction method are as following:

1) Estimate Hurst parameter of the SINR series (denoted as $x(n)$), thus, get value of the differential factor, d.

2) Convert SINR series from F-ARIMA(p, d, q) process to an ARMA(p, q) process (denoted as $w(n)$), as formula:

$$w(n) = \nabla^d(x(n) - \mu) \tag{4.5}$$

where μ is the expected value of $x(n)$. And,

$$\nabla^d = (1 - B)^d = \sum_{k=0}^{\infty} \binom{d}{k} (-1)^k B^k \tag{4.6}$$

here, B is a lag operator, $x(n-1) = Bx(n)$. In addition,

$$\binom{d}{k} = \frac{\Gamma(d+1)}{\Gamma(k+1)\Gamma(d-k+1)} \tag{4.7}$$

where, Γ represents the gamma function.

3) Estimate $\phi(B)$ and $\theta(B)$ of $w(n)$ using Prony method [41].

$$\phi(B) = 1 - \phi_1 B - \phi_2 B^2 - \cdots - \phi_p B^p \tag{4.8}$$

$$\theta(B) = 1 - \theta_1 B - \theta_2 B^2 - \cdots - \theta_q B^q \tag{4.9}$$

4) Convert F-ARIMA(p, d, q) process to F-ARIMA$(0, d, 0)$ process (denoted as $y(n)$) through $y(n) = \theta(B)^{-1}\phi(B)x(n)$

5) Predict one-step ahead value of $y(n)$ by applying formula:

$$\hat{y}(n) = \sum_{j=1}^{k} \beta_{kj} y(n-j) \tag{4.10}$$

where

$$\beta_{kj} = -\binom{k}{j} \frac{\Gamma(j-d)\Gamma(k-d-j)}{\Gamma(-d)\Gamma(k-d+1)} \tag{4.11}$$

6) Compute the predict value of F-ARIMA(p, d, q) process, $x(n)$ according to $\hat{y}(n)$ through $\hat{x}(n) = \theta(B)^{-1}\phi(B)\hat{y}(n)$

Using the method mentioned above, we take the SINR series from node 0 to node 1 of the speed scenario by $U[0, 20](m/s)$ as an example, to do the prediction and show the performance of the prediction method. We predict the one-step ahead value of SINR series by Matlab and compare the predicted values, as shown in Fig.4.2, to the original SINR series, as shown in Fig.4.1. The two figures show that the method is able to accurately predict the value of SINR series so as to track the trend of variation of SINR series.

In addition, we calculate the values of differences between predicted values and original ones (predicted value minus original value) as shown in Fig.4.3. From the figures, it is obvious that the difference values between predicted values and original ones, which may lead to a wrong decision when predicting whether a packet is transmitted successfully, are mostly within the range of $\pm 0.5 \times 10^{-4}$. In order to capture the characteristics of the difference, we estimate the probability density of the difference. The estimation method is that, we separate the range of the difference values into continuous intervals with 1×10^{-6}, which is the accuracy degree of numeric data. And

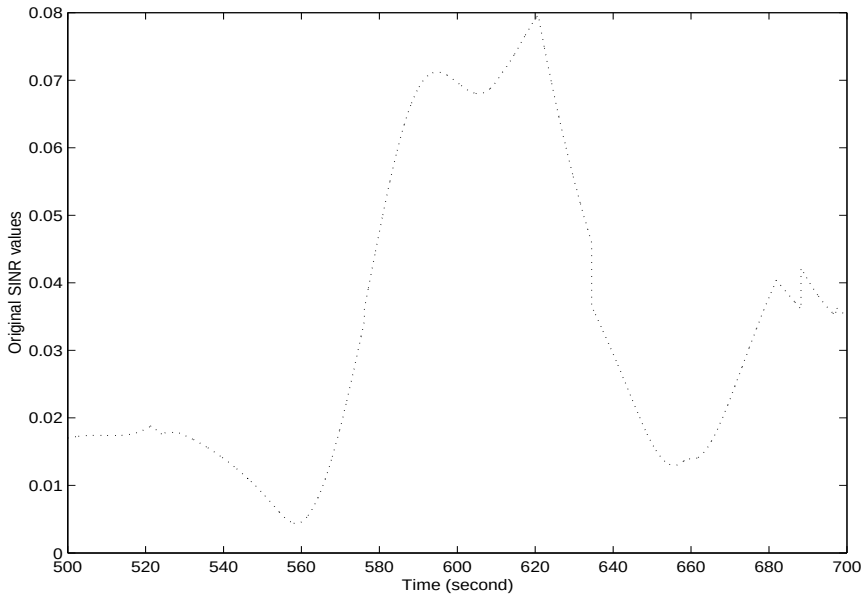

Figure 4.1: Performance of real SINR series

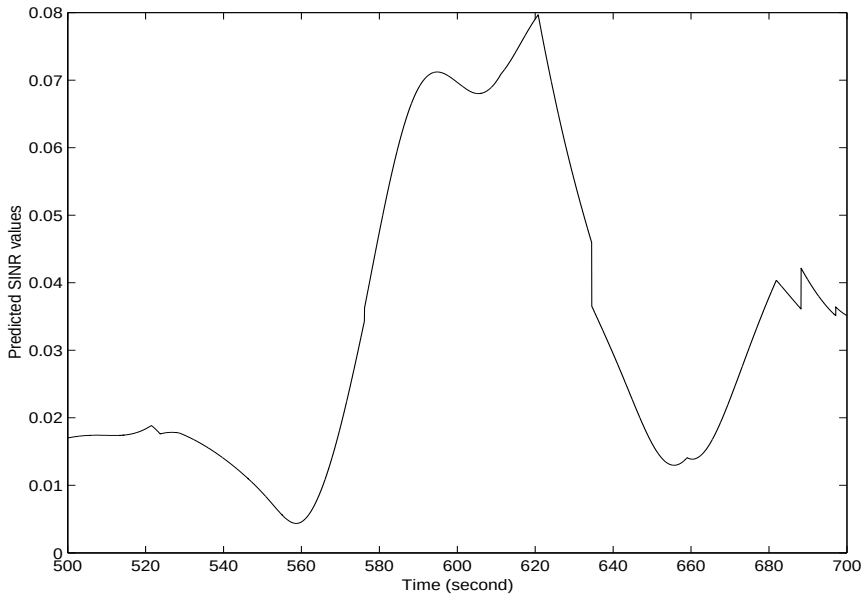

Figure 4.2: Performance of predicted SINR series in one-step ahead

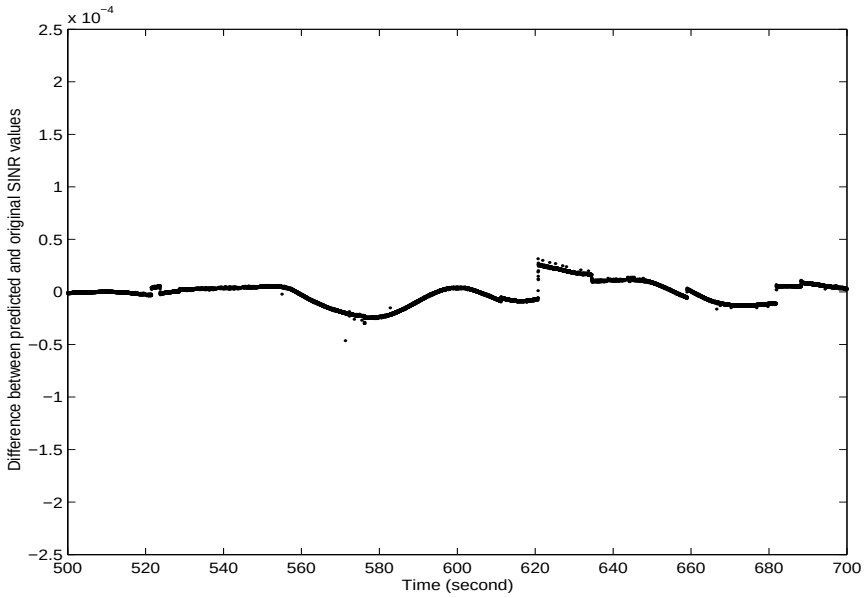

Figure 4.3: Difference between predicted and real SINR values

we count the number of difference values which fall into every interval from all of the data and calculate the probability of an interval as the number of difference values in it minus the total number of data. With the probabilities of these continuous intervals, we can approximate the shape the probability density function (PDF) of the difference, which is shown in Fig.4.4.

Actually, the value of the prediction error is dependent on the prediction method and the number of available history data for prediction. In order to simplify the problem and to focus on improving our scheme of QoS provision, here we present a way to estimate the error in predicting SINR values based on our example data so that the predicted SINR values in later simulation evaluations of our improved scheme can be approximated by the original SINR value plus this estimated error.

From the shape of Fig.4.4, we find that the shape of probability density of all the values of the difference can be approximated by the PDF of a modified normal distribution. Therefore, according to the values in the figure, we propose the following function to

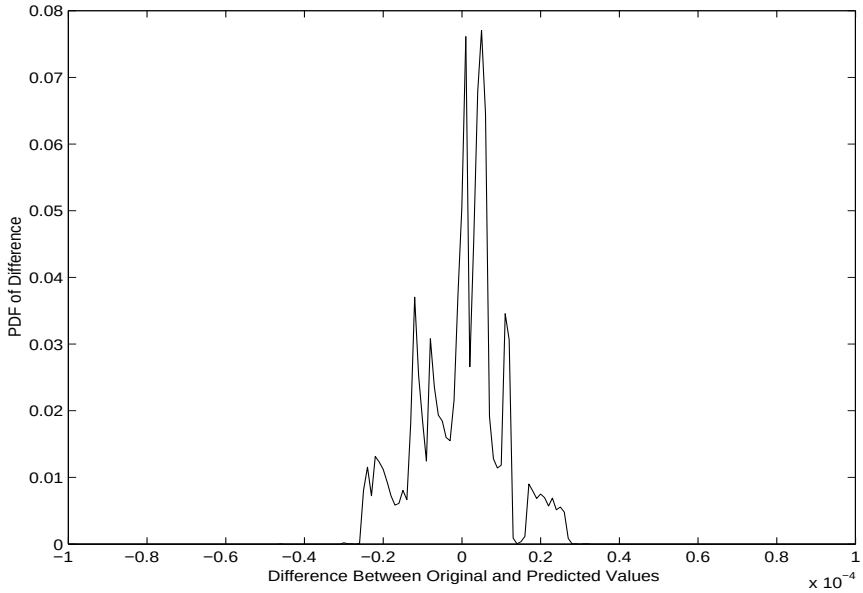

Figure 4.4: Probability density of difference between predicted and real SINR values

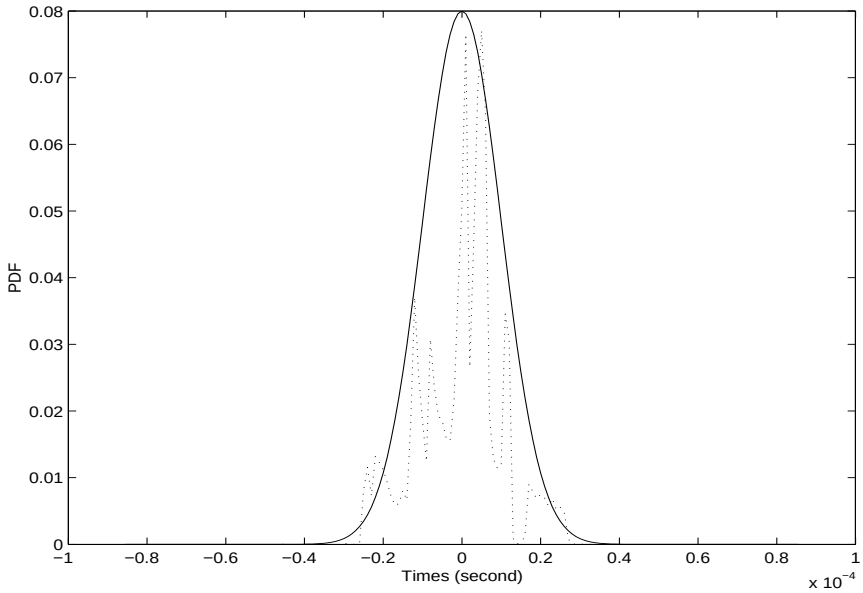

Figure 4.5: PDF of estimation method for difference between predicted and real SINR values

estimate the variance error:

$$\varrho = \frac{1}{\sigma\sqrt{2\pi}} e^{-\frac{(\varepsilon x)^2}{2\sigma^2}} \tag{4.12}$$

here, variance, σ, is 5.0 which makes sure that the probability density is 0.08 at $x = 0$. And ε is 5×10^5, which makes the probability density drop to around 0.01 when x equals to $\pm 2 \times 10^{-5}$. The performance of this estimation method is shown in Fig.4.5.

4.4 An Improvement Scheme: PDMED+

In the previous two sections, we have seen that, based on our proposed SINR model, SINR series can be predicted. Thus, we are able to have the information about time-varying effects of wireless channel on packet transmission due to mobility of nodes. Whether a packet is able to be transmitted successfully can be acquired ahead of its transmission.

With the predicted SINR on packet transmissions in physical layer, now we are going to design an improved scheme of PDMED. In order to simplify our work, we just set the SINR threshold to decide whether a packet is transmitted successfully to receivers, instead of modulation methods. In addition, to focus on scheme design, we assume that our SINR model generates real SINR value. A method to adjust the threshold in order to get correct decision on successful packet transmissions is left for our future work. Thus, in following simulations, the threshold of SINR for deciding successful transmissions is decided arbitrarily. Moveover, for simplifying the expression, in the following, good channel quality means that the SINR is above the threshold, or bad channel for the SINR that is below the threshold.

First, let us look at how PDMED works with mobile nodes moving randomly. In PDMED, when a transmitter node suffers a bad wireless channel quality during trans-

mitting a packet, no matter due to mobility or channel error, it still transmits the packet because it does not know the channel quality. Then, after waiting for a time-out period after transmitting a packet, the transmitter does not receive ACK from the receiver node and assumes that it fails to transmit the packet due to collisions. Then the transmitter node will double its contention window size, generate a back-off duration and start to back off in order to retransmit the packet. However, indeed, there is no collision happening, just a bad channel quality. It is wasteful for the transmitter node to back off again with a doubled contention window. Getting this insight, we proposed a simple modification of PDMED, namely PDMED+, as following.

When a transmitter node is going to transmit a packet, it predicts the SINR that the packet will suffer in the point of view at the receiver node and decides whether the packet is able to be successfully transmitted or not according to a threshold to SINR. If the node predicts that the transmission will fail, it defers the packet's transmission until the environment makes SINR the packet will suffer be over the threshold, i.e. the channel turns to be good and the packet is able to be successfully transmitted.

However, this method also has two drawback situations. First, if the channel is bad for such a longer time than the total duration of retrying seven times in IEEE 802.11, the delay of a packet is increased tremendously. However, in PDMED which is based on retransmission algorithm in IEEE 802.11, the packet will be dropped if it is not able to transmit successfully after seven retransmissions. Therefore, the delay of a packet is controlled with an upper limit. Second, when there are two nodes deferring itself waiting for good channel, during their deference period, there is one of their neighboring transmitters successfully transmits a packet. During the period of the transmission, the channel becomes good for both of the two deferring nodes. After the transmission finishes, two deferring nodes will begin to transmit their packets at the same time.

At this time, collision happens definitely. Two nodes have to double their contention windows and back off for retransmission.

We proposed the following methods to handle above mentioned drawbacks. In order to overcome the first drawback, we also set a limit period for deferring a packet transmission because of bad channel quality. Borrowing the retransmission mechanism in IEEE 802.11, we set the similar long time for the total deferring period as:

$$T = 2^7 \times W_{min} \times \delta \tag{4.13}$$

where, δ is the slot time. After the time, the packet is dropped.

For the second drawback, when two deferring nodes predict good channel quality after hearing a transmission, we give differentiated periods for the two nodes before they transmit the deferred packets. We set the differentiated period as following formula:

$$\sigma_i = U[0, r_i \times W_{min}] \times \delta \tag{4.14}$$

where $U[x, y]$ is a uniform distribution function that generates random integer numbers within the range $[x, y]$. σ_i is the time for differentiated period of flow i. r_i is the rank of flow i. W_{min} is the minimum contention window size of all flows. δ is the slot time. This improvement scheme, PDMED+, is illustrated in Fig. 4.6.

Compared to PDMED, PDMED+ can definitely contribute benefits in the following situations: 1) When a packet is going to be transmitted at a node, the channel quality is bad (i.e. the SINR that it will suffer is below the threshold). Then, the channel quality will become good soon (e.g. the next time slot immediately) before the end of back off period if the node takes a retransmission action in PDMED. In this situation, PDMED+ will transmit the packet earlier than PDMED and help to reduce the delay that the packet suffers. 2) When a packet is going to be transmitted at a node, the

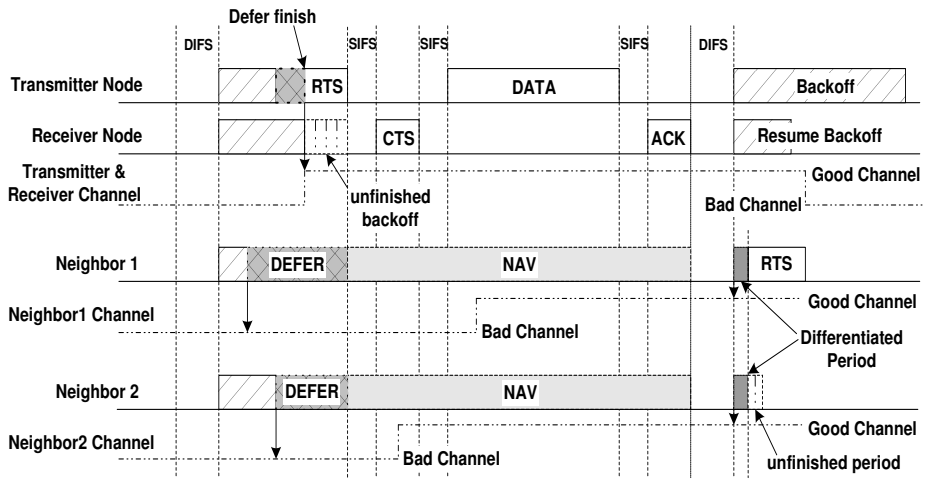

Figure 4.6: Illustration of the methods in PDMED+

channel quality is bad. In PDMED, the node will transmit the packet no matter how because the transmitter node does not know whether the packet will be transmitted successfully. Then, the shared wireless medium is occupied by this failed transmission. However, in PDMED+, the node will hold on its transmission and leave the wireless medium for other nodes. If at this time, there is another neighboring transmitter node which has a packet to transmit and has a good channel, it is able to utilize the shared wireless channel and transmit a packet. Thus, the total throughput of the network can be increased.

4.5 Performance Evaluation

We evaluated PDMED+ by simulations using OPNET as well. The topology shown in Fig. 3.12 is also used. Two flows, flow 1($S1 \rightarrow D1$) and flow 2($S2 \rightarrow D2$), are transmitted in the network as illustrated in Fig. 3.12. All the nodes move according to Random Waipoint model. The AODV routing protocol is adopted. We also adopt the video traces of movie, Jurassic Park, as the traffic for evaluation, which is coded by H.263 at 265 kbps. The large packets whose sizes are over 2000 bytes are fragmented

into several fragments with 2000 bytes and the residual bytes. Two flows adopt the same video trace, but with the different off-set of starting time. The off-set times of flow 1 and 2 are 0 and 300 seconds respectively. In addition, we fix the differentiation ratio between flow 1 and 2 at 1.0 : 2.0 in all of simulation scenarios, i.e. $\phi_2/\phi_1 = 2$. And, we define the ratio of average end-to-end delays between two flows as D_2/D_1, which D_2 is average end-to-end delay of flow 2 and D_1 is average end-to-end delay of flow 1. In MAC layer, W_{min} and W_{max} are fixed at 16 and 1024 time slots, respectively. The duration of each time slot, $T_{slot} = 20\mu s$ seconds. In following figures, F1 denotes flow 1 and F2 denotes flow 2.

In order to make sure that the following comparisons for evaluations are under the same mobility conditions, we first record the trajectories of all the nodes which move in random waypoint model with a sampling interval of 0.01 second for five different speed scenarios ($U[0, 20]$, $U[0, 40]$, $U[0, 60]$, $U[0, 80]$, $U[0, 100]$) by simulations. The results are saved into a file for every node in every speed scenario. In all of the following simulation experiments, all the nodes read their files and move according to their recorded trajectories respectively so that the comparison experiments of our scheme between different settings can be conducted under the same situation of mobility of nodes. We also recorded the SINR series according to mobility into a file for every node (as a receiver node) in every speed scenario with the sampling interval, 0.01 second. In addition, the threshold for deciding the channel quality according SINR values is just chosen at will as long as it makes sure that the channel quality experiences some time of bad quality. Thus, for all nodes, the thresholds chosen in our following simulations are 0.04, 0.018, 0.006, 0.06 and 0.015 respectively for the speed scenarios of $U[0, 20]$, $U[0, 40]$, $U[0, 60]$, $U[0, 80]$ and $U[0, 100]$.

4.5.1 Benchmark to PDMED

First we evaluate PDMED+ with ideal SINR information, which benchmark to PDMED with the nodes moving by Random Waypoint model. The transmitter node reads the SINR files of its receiver node and acquire SINR value with the same interval as the sampling interval so that it gets the ideal SINR values.

Fig.4.7 shows the comparison on average end-to-end packet delay between two schemes. We can see that, in all of the speed scenarios, the average end-to-end packet delays of PDMED+ are roughly close to the average end-to-end packet delays in PDMED. That means, even though we defer the packet transmissions when channel is bad, PDMED+ does not increase much of the average end-to-end delay and sometimes achieves the smaller average end-to-end delay, compared to the performance of PDMED. In the scenarios of $U[0, 20]$, $U[0, 40]$ and $U[0, 100]$, the average end-to-end delays of PDMED+ are a little bit higher than those of PDMED. But in the scenarios of $U[0, 60]$ and $U[0, 80]$, PDMED+ achieves the smaller average end-to-end delays.

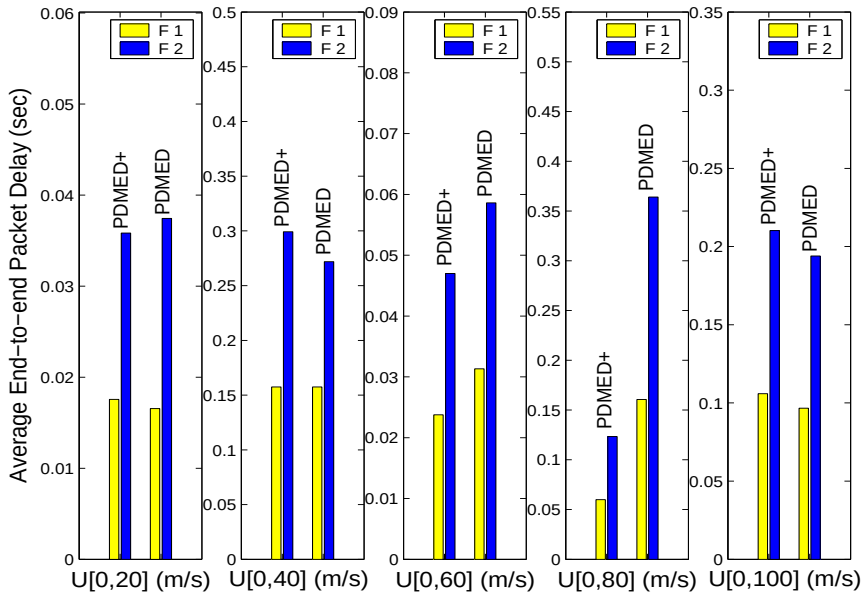

Figure 4.7: Average end-to-end delay by different speed scenarios

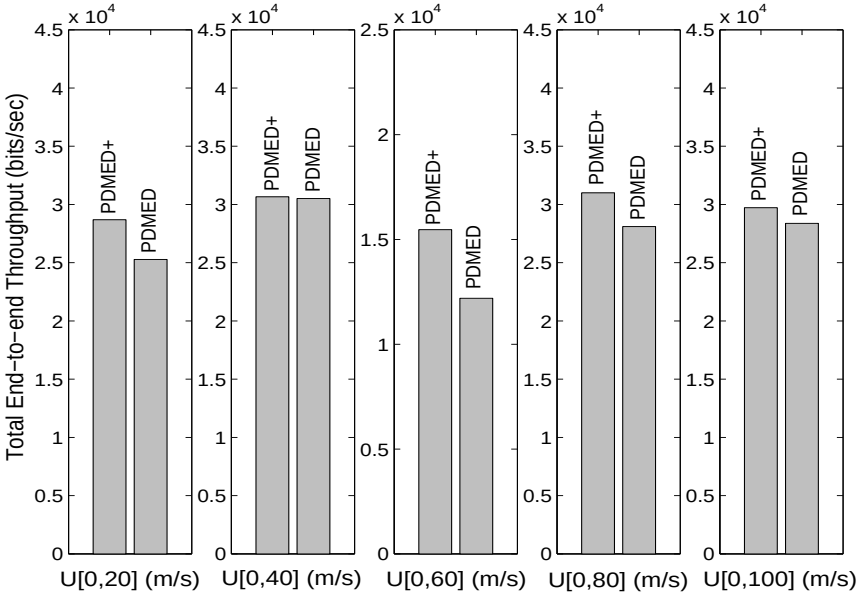

Figure 4.8: Total throughput by different speed scenarios

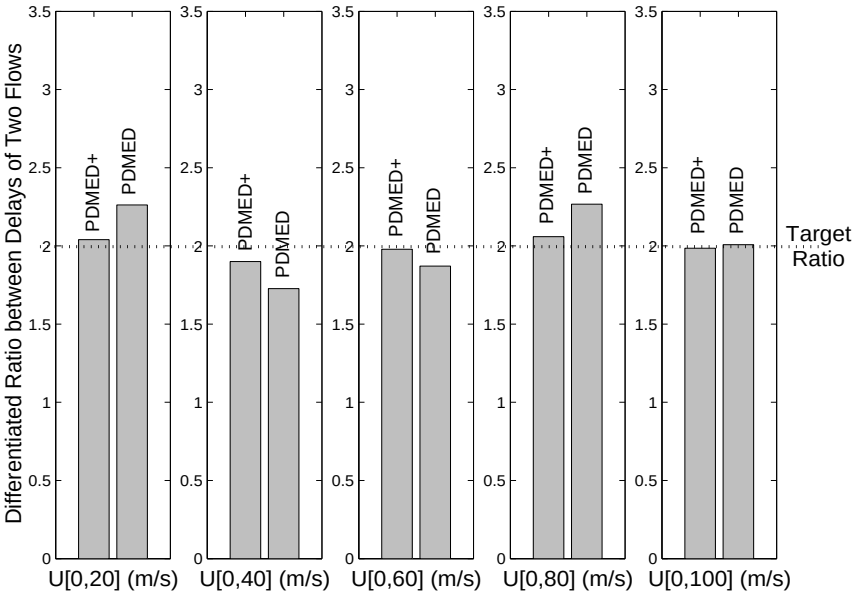

Figure 4.9: Ratios of average end-to-end delay between flows by different speed scenarios

Fig.4.8 shows the total throughput of two flows of two realizations. From the figure, it is obvious that PDMED+ is able to increase the total throughput of two flows, compared to PDMED. This confirms that compared to retransmission method in PDMED, the way of deferring the packet until the channel becomes good in PDMED+ is able to utilize the channel ability more efficiently. Although PDMED+ may increase a little bit of average end-to-end delay sometimes, it achieves more accurate differentiated ratio (D_2/D_1) between two flows as shown in Fig.4.9. In the figure, the achieved ratio of PDMED+ is closer to the line of target ratio ($\phi_2/\phi_1 = 2$), compared to PDMED. The reason is that more packets are able to be transmitted by PDMED+ so as to increase the chances to adjust the differentiation ratio between two flows.

4.5.2 Packet Expiry Policy

After evaluating the overall performance of PDMED+, we now study the usefulness of the expiry policy in PDMED+. We disable the expiry policy in PDMED+ so that it only defers packets when meeting bad channel quality until the channel becomes good. Then, through simulations, we compared the performance of PDMED+ without expiry policy to that of the normal PDMED+.

In Fig.4.10, which shows the comparison of the average end-to-end delay of two flows, we can see that without the policy, the average end-to-end packet delay increases. The result confirms that the expiry policy does help to avoid packets being deferred too long time in order to wait for a good channel when meeting the situation that the channel becomes bad for a long time. It controls packet delay and drops the useless packets which are delayed too long time so that network resources are saved for upcoming packets. It also helps to reduce queuing delay of packet in queues due to a long-delayed HOL packet which waits for good channel quality.

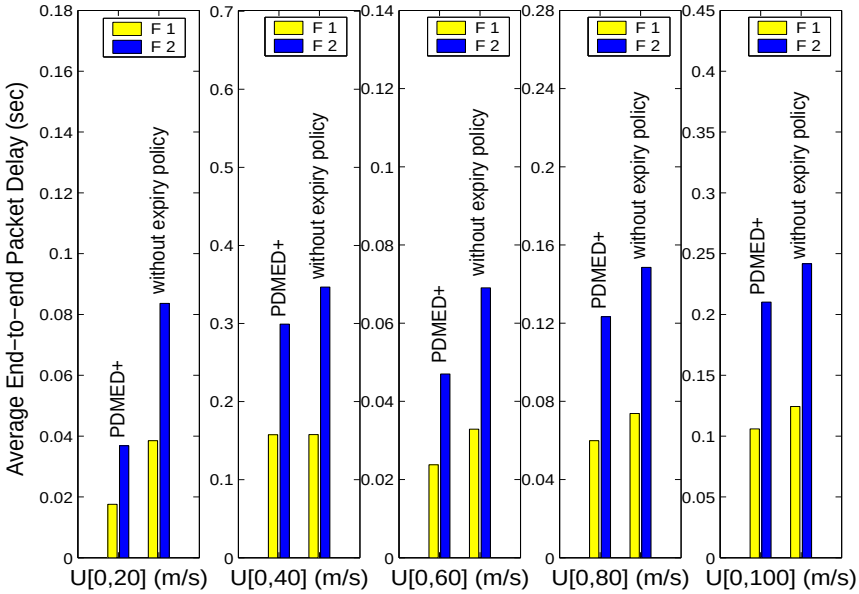

Figure 4.10: Average end-to-end delay with/without expiry policy by different speed scenarios

Although expiry policy has no differentiated parameters, it does not destroy the proportional differentiation performance, as illustrated in Fig.4.11. In the figure, four scenarios among all five scenarios ($U[0,20]$, $U[0,40]$, $U[0,60]$, $U[0,100]$), exhibit that the normal PDMED+ achieves closer differentiated ratio to target ratio compared to PDMED+ without expiry policy. Even in the speed scenario of $U[0,80](m/s)$ in which the ratio of normal PDMED+ deviate a little bit larger than the ratio of PDMED+ without expiry policy, the value of achieved ratio of normal PDMED+ is still close to the target ratio.

Fig.4.12 shows that expiry policy does not have any obvious good or bad performance on total end-to-end throughput of two flows between the normal PDMED+ and PDMED+ without expiry policy. In the scenarios with the speeds of $U[0,20]$, $U[0,80]$ and $U[0,100]$, PDMED+ without expiry policy achieves less total throughput than the normal PDMED+, whereas it achieves better total throughput than the normal PDMED+ in the scenarios with speeds of $U[0,40]$ and $U[0,60]$. The reason is that,

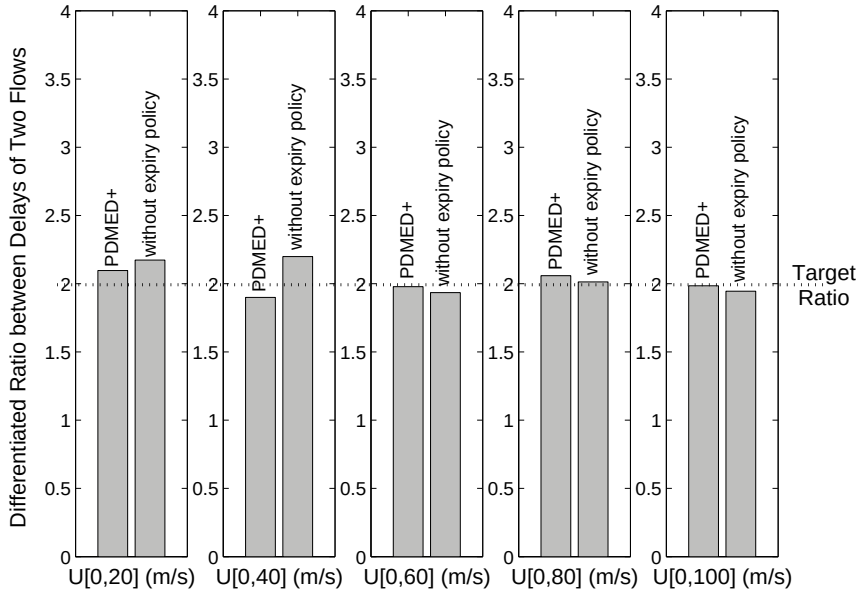

Figure 4.11: Ratios of average end-to-end delay between flows with/without expiry by different speed scenarios

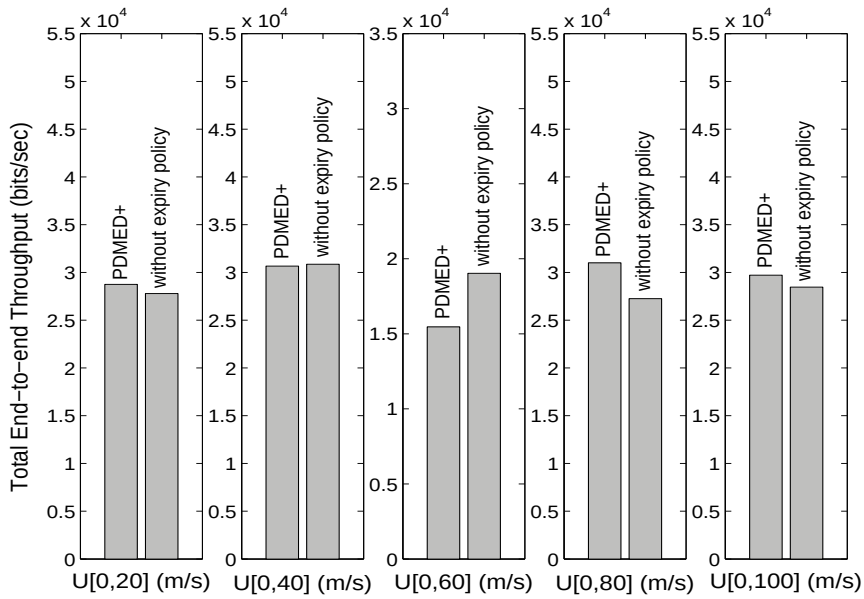

Figure 4.12: Total throughput with/without expiry by different speed scenarios

expiry policy drops packets that are deferred for a too long time so that less packets reach the destination nodes, but it also saves network resources for other packet transmissions so that the throughput of other flows may be increased. In addition, when the channel remains bad for a long time, without expiry policy, deferring transmission of packets may lead to a deadlock of a flow so as to sacrifice its throughput. However, if the period of the bad quality channel is just a little longer than the expiry period, PDMED+ without policy finally transmits the packet successfully, whereas the normal PDMED+ will drop the packet and back off to prepare for next transmission. In this situation, PDMED+ without expiry policy may increase the throughput of a flow. Thus, the effect of expiry policy on total throughput is dependent on the situation of network.

4.5.3 Differentiated Period Policy

In this section, we evaluate the usefulness of differentiated period policy through simulations using the same method as expiry policy. We disable the differentiated period policy and compared its performance to that of the normal PDMED+.

In Fig.4.13, we can see that the average end-to-end packet delay of PDMED+ without differentiated period is larger than or almost the same as that of the normal PDMED+ in the speed scenarios of $U[0, 20]$, $U[0, 60]$ and $U[0, 80]$, but lower in the speed scenarios of $U[0, 40]$ and $U[0, 100]$. This result exhibits that the differentiated period policy does reduce the possibility of collision between neighbor nodes when they begin to transmit in a good period after a neighboring transmission most of time. However, if no such kind of collisions happened, this differentiated period is a delay overhead, although it is a short time. This is why we see the differentiated period may increase a little on the average end-to-end packet delay. However, in overall, the results show that the

differentiated period contributes relevantly larger benefits and less harm on the average end-to-end packet delay.

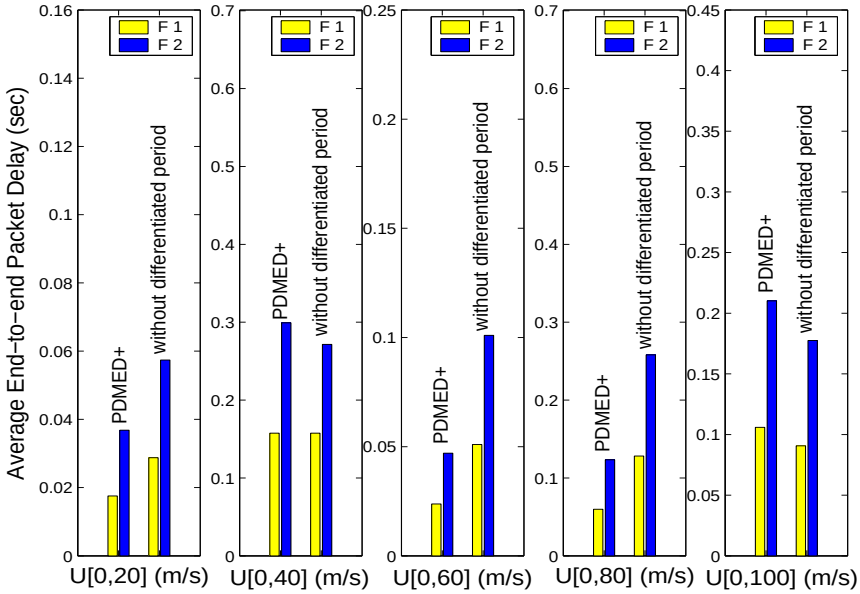

Figure 4.13: Average end-to-end delay with/without differentiated period policy by different speed scenarios

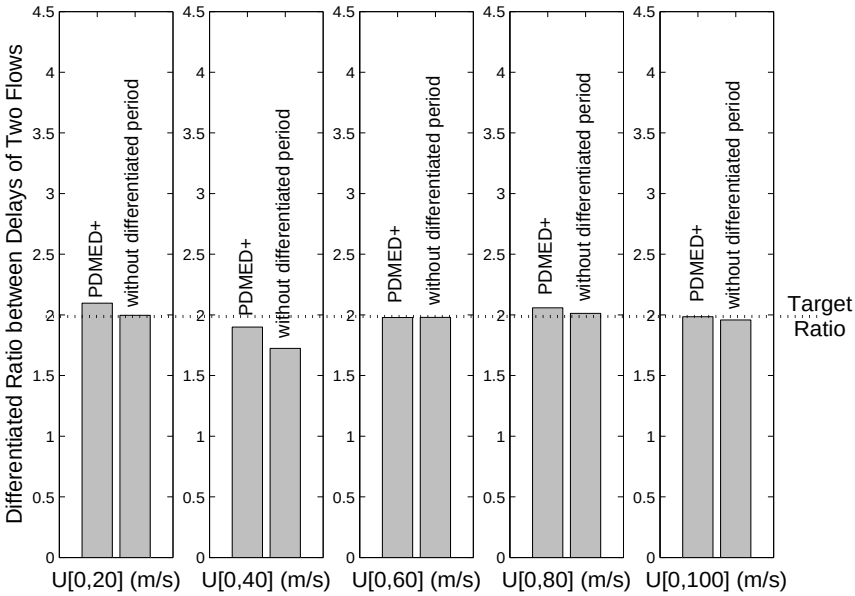

Figure 4.14: Ratios of average end-to-end delay between flows with/without differentiated period policy by different speed scenarios

For achieved differentiation ratio, the differentiated period has no definite good or bad

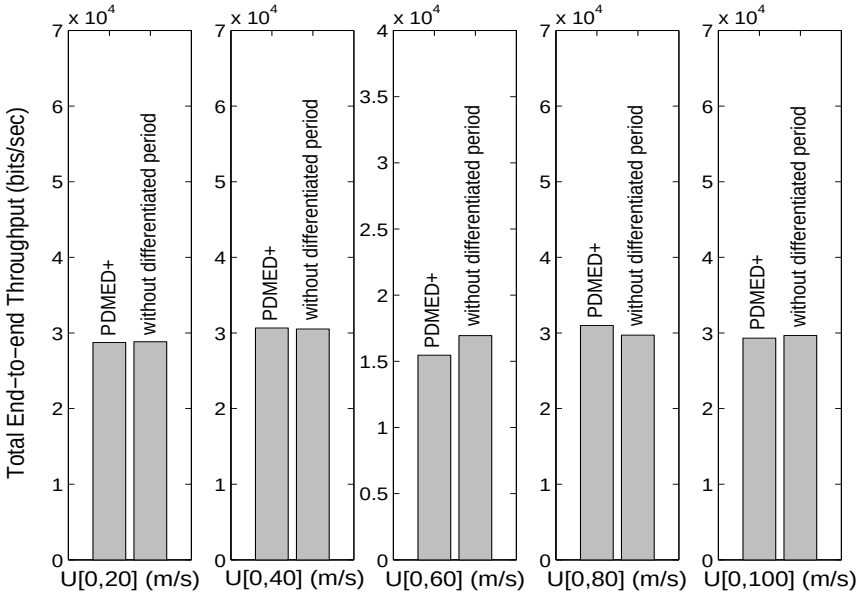

Figure 4.15: Total throughput with/without differentiated policy by different speed scenarios

contributions on the accuracy of achieved differentiated ratio between two flows as shown in Fig.4.14. In the figure, the ratio of PDMED+ deviates larger from the target ratio than PDMED+ without differentiated period policy in the speed scenarios of $U[0, 20]$, $U[0, 80]$. In the other three scenarios, the normal PDMED+ achieves more accurate ratios. However, in overall, the achieved ratios of the normal PDMED+ are close to our target ratios. Thus, we can say that the differentiated period does not have much effect on the accuracy of achieving our proportional differentiation.

In Fig.4.15, we also do not see any obvious contribution of the differentiated period policy on total end-to-end throughput of two flows. In the scenarios with the speeds of $U[0, 20]$, $U[0, 40]$ and $U[0, 100]$, the normal PDMED+ and PDMED+ without differentiated period policy have almost the same throughput. In the scenario with speed of $U[0, 60]$, the normal PDMED+ achieves less throughput than PDMED+ without differentiated period policy does, whereas the normal PDMED+ achieves more throughput in the scenario with speed of $U[0, 80]$. So the differentiated period policy also does not

affect total throughput of network.

4.5.4 PDMED+ with Predicted SINR

Finally, we evaluate the performance of PDMED+ with the predicted SINR value by the suggested prediction method. As we mentioned in Section 4.3, we approximate the predicted SINR values through adding estimated error on accurate SINR values in our simulations. The estimation method as mentioned in (4.12) generates the random error values for SINR value which is roughly consistent with the shape of probability density of the difference between original and estimated SINR generated by our suggested prediction method. We focus on evaluating the effect generated by the error of predicted SINR on the performance of PDMED+.

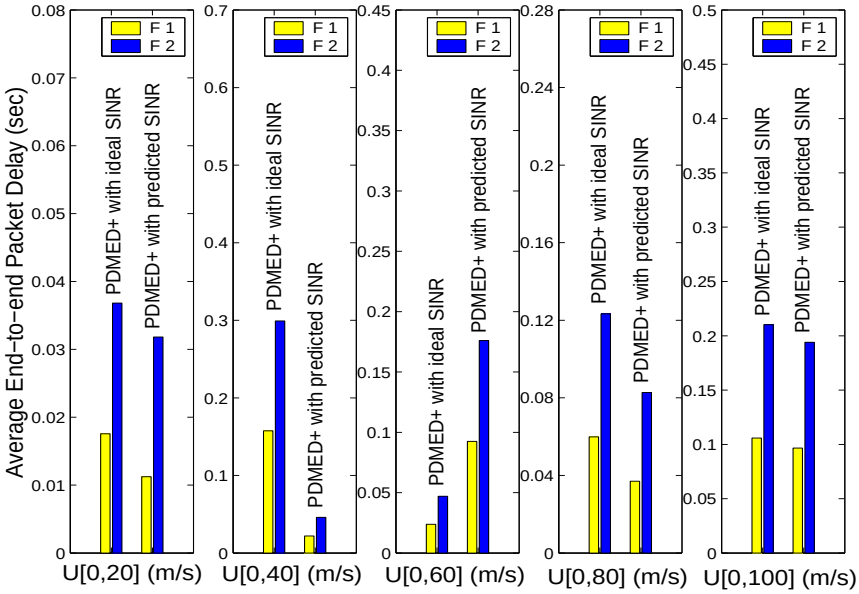

Figure 4.16: Average end-to-end delay with ideal SINR and predicted estimated prediction by different speed scenarios

Fig.4.16 shows the comparison on the average end-to-end packet delay between PDMED+ with ideal SINR and predicted SINR. We can see that although the estimated error of the predicted SINR is very small, it still affects the average end-to-end delays dif-

ferently in different speed scenarios. In the scenario with speed of $U[0, 20]$, $U[0, 40]$, $U[0, 80]$ and $U[0, 100]$, the average end-to-end delay of PDMED+ with ideal predicted SINR is larger than that of PDMED+ with estimated predicted values. In the scenario with speed of $U[0, 60]$, the results are opposite. Thus, according to our experiment data, the error of prediction method generates some variation of the average end-to-end delay, compared to PDMED+ with ideal SINR values. And, time-varying wireless channel due to mobility and random access method of MAC protocol also enlarges the variation.

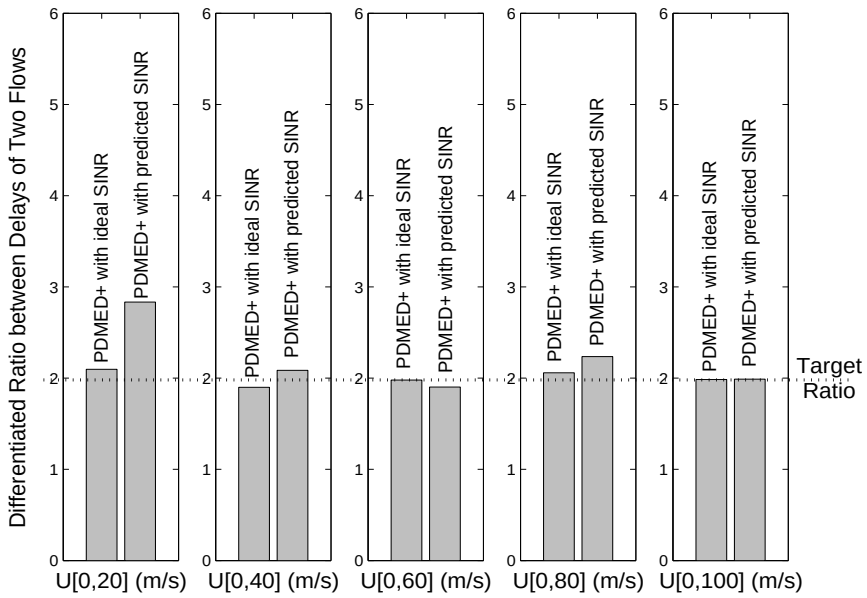

Figure 4.17: Ratios of average end-to-end delay between flows with ideal and estimated prediction by different speed scenarios

Diverse effects are also shown in differentiated ratio on average end-to-end delay between two flows, as illustrated in Fig.4.17. Compared to PDMED+ with ideal SINR values, PDMED+ with predicted SINR values achieves less accurate differentiated ratios. This is also because of the variation on average end-to-end delay that estimated error generates. And, in the scenario with speed of $U[0, 20]$, the ratio of PDMED+ with predicted SINR values deviates far from the line of target ratio because the data are

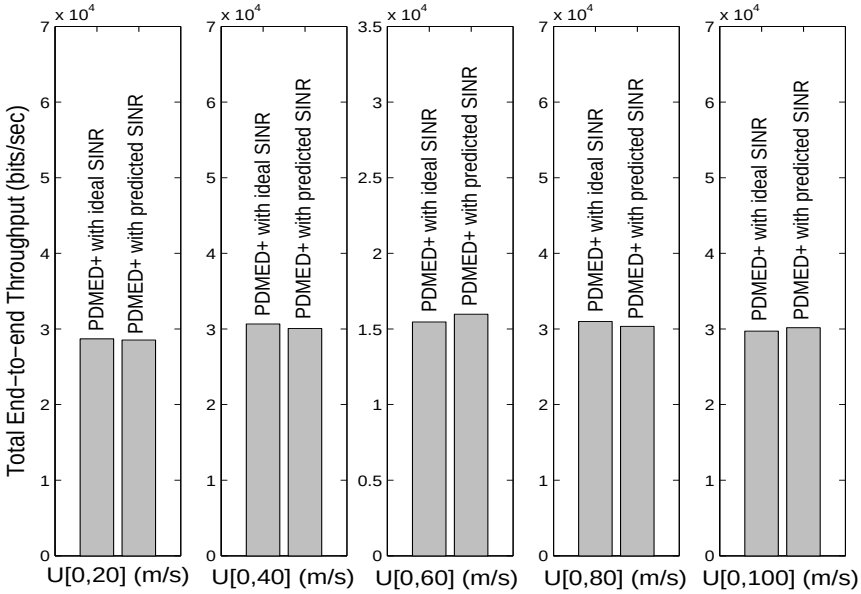

Figure 4.18: Total throughput with ideal and estimated prediction by different speed scenarios

collected at the time when difference of normalized average end-to-end delay becomes large. But overall, in all the scenarios, the ratios of PDMED+ with predicted SINR values deviate farther from the target ratio than PDMED+ with ideal SINR values.

Finally, Fig.4.18 shows the performance of total throughput of two flows. In all of the scenarios, the total throughput of PDMED+ with ideal SINR is close to that of PDMED+ with predicted SINR. This means that the error of SINR value generated by prediction method does not effect total throughput of two flows. Therefore, PDMED+ using predicted SINR is also able to improve the total throughput in the environment with nodes' mobility.

4.6 Conclusions

With the motivation of improving the performance of PDMED in the environment with mobile nodes and time-varying wireless channel, we studied the characteristic of SINR in wireless multi-hop ad hoc network based on CSMA/CA access protocol. We pro-

posed a simple model to analyze the SINR between any two nodes in a network in which nodes move freely in random waypoint model. Through our study, we found the SINR between any two nodes exhibit self-similar characteristics. Based on our discovery, we suggested a prediction method which is able to predict accurate SINR value so as to function as a channel monitor to provide transmission information in physical layer for distributed scheduler on proportional differentiation provision. And, we also proposed an improvement of PDMED, namely PDMED+, to utilize the information from the channel monitor to achieve better performance in wireless multi-hop ad hoc network. Through random event simulations, the results prove that PDMED+ achieves better total end-to-end throughput while it still maintains a good proportional differentiation on average end-to-end packet delay in the network in which nodes move by random waypoint model.

Chapter 5

Conclusions and Future Works

5.1 Conclusions

Wireless multi-hop ad hoc networks which are demanded by more and more applications with different QoS requirements suffer from time-varying and limited network resources. Thus, it is not easy to deploy QoS provisions to satisfy the expectations of all users. An efficient network allocation between users according to their end-to-end QoS performances would be desirable. Due to the time-varying characteristic of network topology and wireless link capacity, several network components have to cooperate to achieve this kind of optimization.

This thesis first contributed a cross layer framework to provide a conception of providing proportional differentiation on end-to-end performances of users in wireless multi-hop ad hoc networks. Through four mechanisms in different layers and three monitors, the necessary information is exchanged between layers and adapts the functions of different network components so as to achieve proportional differentiation on end-to-end performance between users.

After proposing the framework, a realization, PDMED, was contributed to focus on

designing a mechanism to provide a consistent and accurate proportional differentiation on the average end-to-end delay based on CSMA/CA medium access. Specifically, the distributed scheduler dynamically adjusts the backoff duration of a flow based on its instantaneous deviation from the maximum average end-to-end packet delay. QoS monitor functions via a feedback method and information sharing due to broadcasting wireless medium together with the store-and-forward multi-hop transmission. The destination nodes feedback its instantaneous average end-to-end packet delay along the transmission path in backward. And neighbor nodes along the path monitor the feedback information. Rich random event simulations have been done to evaluate the performance of PDMED and prove the ability of the realization to achieve a consistent and accurate proportional differentiation on end-to-end packet delay in wireless multi-hop ad hoc network when the node density of network is not low.

However, time-varying network topology and wireless link capacity due to mobility of nodes reduce network resource utilization while providing QoS in wireless ad hoc networks. In order to monitor the time-varying effects on packet transmissions due to wireless channel quality and increase utilization efficiency of the wireless channel capacity, we studied the characteristic of SINR between any two nodes in CSMA/CA based wireless multi-hop ad hoc networks and contributed to a discovery that SINR between two nodes in multi-hop ad hoc network under random waypoint model exhibits self-similarity. Based on our discovery, a channel monitor method is suggested to predict the SINR by one-step ahead. After that, we proposed an improvement scheme, PDMED+, cooperating to channel monitor to increase the total throughput of the network, while maintaining the proportional differentiation on average end-to-end delay. Through simulation evaluations, we indeed see an improvement on total throughput of the network. Although PDMED+ costs a little extra average end-to-end packet delay,

it still maintains a good consistent and accurate proportional differentiation on average end-to-end packet delay.

5.2 Future Works

Because PDMED and PDMED+ cannot function well if nodes suffer long time of re-routing a new path when the density of nodes in network is low, how to guide the density of nodes in network is necessary to study. With the same objective, a method to guide the movement of the nearby nodes which have no traffic load to breaking link area so as to quickly recover the link is also valuable to study.

In addition, considering dynamically varying network conditions, an adaptive QoS routing protocol is also necessary to reduce the cost of re-routing and cooperate to scheduler to deliver packets faster. And an admission control may also provide cooperation help to achieve proportional differentiation when it is necessary.

In addition, in our model of studying signal-to-noise ratio in CSMA/CA based multi-hop ad hoc network, the interference is adopted at an upper bound. The future work has to design a method that can use this upper bound value to approximate the real SINR values so as to reflect the real instantaneous situation of packet transmissions in physical channels. In addition, it is also meaningful to research on how to utilize the SINR information to support proactive routing.

Bibliography

[1] I. F. Akyildiz, W. Su, Y. Sankarasubramaniam, E. Cayirci. A Survey on Sensor Networks. *IEEE Communications Magazine*, August 2002.

[2] IEFT Mobile Ad hoc Network working group charter. Description of working group. *http://www.ietf.org/html.charters/manet-charter.html*, Februry 2000.

[3] M. S. Corson. Issues in supporting quality of service in mobile ad hoc networks. *In IFIP 5th Int. Workshop on Quality of Service-(IWQOS'97)*, May 1997.

[4] I. Chlamtac, A. Farago, Making transmission schedules immune to topology changes in multi-hop packet radio networks. In *IEEE/ACM Transactions on Networking (TON)*, Pages:23-29, Volume 2, Issue 1. February 1994.

[5] J. Ju, V. O. K. Li, An optimal topology-transparent scheduling method in multi-hop packet radio networks. In *IEEE/ACM Transactions on Networking (TON)*,Pages:298-306, Volume 6, Issue 3. June 1998.

[6] J. L. Sobrinho, A. S. Krishnakumar, Quality of service in ad hoc carrier sense multiple access wireless networks. *In IEEE JSAC*, August 1999.

[7] J. Sheu, C. Liu, S. Wu, Y. Tseng, A priority MAC protocol to support real-time traffic in ad hoc networks. In *ACM Wireless Networks*, Pages:61-69, Volume 10, Issue 1, January 2004.

[8] X. Yang, N. H. Vaidya, Priority scheduling in wireless ad hoc networks. In *Proceedings of the 3rd ACM international symposium on Mobile ad hoc networking and computing*, Pages:71-79, 2002.

[9] I. Aad, C. Castelluccia, Differentiation mechanisms for IEEE 802.11. In *Proceedings of IEEE Infocom 2001*, Anchorage-Alaska, April 2001.

[10] J. Zhao, Z. Guo, Q. Zhang, W. Zhu, Performance study of MAC for service differentiation in IEEE 802.11. *IEEE Globecom02*, 2002.

[11] M. Benveniste, G. Chesson, M. Hoehen, A. Singla, H. Teunissen, M. Wentink, EDCF proposed draft text, *IEEE working document 802.11-01/131 rl*, March 2001.

[12] J. Kim, C. Kim, Performance analysis and evaluation of IEEE 802.11e EDCF. In *Wireless Communications and Mobile Computing*, 2004.

[13] B. Li, R. Battiti, Performance analysis of an enhanced IEEE 802.11 distributed coordination function supporting service differentiation. In *QofIS 2003*, LNCS 2811, Pages:152-161, Springer-Verlag Berlin, 2003.

[14] C. Dovrolis, D. Stiliadis, P. Ramanathan, Proportional differentiated services: delay differentiation and packet scheduling. *IEEE/ACM Transactions on Networking*, 10(1):12-26, February 2002.

[15] H. Luo, S. Lu. A topology-independent fair queueing model in ad hoc wireless networks. In *Proceedings of IEEE ICNP'00*, pages 325-335, Osaka, Japan, November 2000.

[16] H. Luo, S. Lu, V. Bharghavan, A new model for packet scheduling in multihop wireless networks. In *Proceedings of ACM MOBICOM 2000*, pages 76-86, August 2000.

[17] H. Luo, S. Lu, V. Bharghavan, J. Cheng, G. Zhong, A packet scheduling approach to QoS support in multi-hop wireless networks. *Mobile Networks and Applications*, Pages:193-206, Volume 9, Issue 3, June 2004.

[18] A. K. Somani, J. Zhou. Achieving fairness in distributed scheduling in wireless ad-hoc networks. In *Proceedings of IEEE International Performance, Computing, and Communications Conference (IPCCC)*, Pages:95-102, April 2003.

[19] J. Chen, A. K. Somani. Fair scheduling in wireless ad hoc networks of location dependent channel errors. In *Proceedings of IEEE International Performance, Computing, and Communications Conference (IPCCC)*, Pages:103-110, April 2003.

[20] V. Kanodia, C. Li, A. Sabharwal, B. Sadeghi, E. Knightly, Ordered packet scheduling in wireless ad hoc networks: mechanisms and performance analysis. In *Proceedings of the 3rd ACM international symposium on Mobile ad hoc networking and computing*, Pages:58-70, Lausanne, Switzerland, 2002.

[21] C. R. Lin, M. Gerla, MACA/PR: An asynchronous multimedia multihop wireless networks. In *Proceedings of IEEE INFOCOM'97*, 1997

[22] V. Kanodia, C. Li, A. Sabharwal, B. Sadeghi, E. Knightly, Distributed priority scheduling and medium access in ad hoc networks. In *ACM Wireless Networks*, Pages:455-466, Volume 8, Issue 5, September 2002.

[23] K. Wang and P. Ramanathan, End-to-end Delay Assurances in Multi-hop Wireless Local Area Networks. In *Proceedings of IEEE Globecom*, 2003.

[24] K. Wang and P. Ramanathan, End-to-end Throughput and Delay Assurances in Multi-hop Wireless Hotspots. In *Proceedings of the 1st ACM international workshop*

on Wireless mobile applications and services on WLAN hotspots, Pages:93-102, San Diego, CA, USA. 2003.

[25] Y. Yang, R. Kravets, Distributed QoS guarantees for realtime traffic in ad hoc networks.In *The First IEEE International Conference on Sensor and Ad hoc Communications and Networks*, SECON, 2004.

[26] D. Schafhuber, G. Matz, MMSE and Adaptive Prediction of Time-Varying Channels for OFDM Systems, *IEEE Transactions on wireless communications*, Vol 4, No.2, 2005.

[27] Y. Zhou, P. C. Yip, H. Leung, On the Efficient Prediction of Fractal Signals, *IEEE Transactions on signal processing*, Vol 45, pp.1865-1868, 1997.

[28] Peng-Yong. Kong, Keng-Hoe Teh, Performance of Proactive Earliest Due Date Packet Scheduling in Wireless Networks. *IEEE Transactions on vehicular technology*, Vol 53, No.4, 2004.

[29] T. Liu, P. Bahl, I. Chlamtac, Mobility Modeling, Location Tracking, and Trajectory Prediction in Wireless ATM Networks. *IEEE Journal on Selected Areas in Communications*, 16, 922-936, 1998.

[30] X. Shen, J. W. Mark, J. Ye, User Mobility Profile Prediction: An Adaptive Fuzzy Inference Approach. *Wireless Networks*, 6, 363-374, 2000.

[31] S. Capkun, M. Hamdi, J. Hubaux, GPS-free Positioning in Mobile Ad Hoc Networks. *System Sciences, 2001. Proceedings of the 34th Annual Hawaii International Conference*, pp.10, Jan, 2001.

[32] R. Hekmat, P. V. Mieghem. Interference in Wireless Multi-Hop Ad Hoc Networks and its Effect on Network Capacity. *Wireless Networks*, Vol 10, Issue 4, July, 2004.

[33] B. G. Chun, M. Baker, "Evaluation of Packet Scheduling Algorithms in Mobile Ad Hoc Networks", In *Mobile Computing and Communications Review*, Volume 1, Number 2, June, 2002.

[34] T. Camp, J. Boleng, V. Davies. A Survey of Mobility Models for Ad Hoc Network Research. *Wireless Communication and Mobile Computing (WCNC): Special issue on Mobile Ad Hoc Networking: Research, Trends and Applications*, vol.2, no.5, pp.483-502, 2002.

[35] Theodore S.Rappaport. Wireless Communications: Principles and Practice. Second Edition.

[36] H. F. Zhang, Y. T. Shu, O. Yang. Estimation of Hurst Parameter by Variance-Time Plots. *Proceedings of the IEEE Pacrim 1997*, pp.883-886, August, 1997.

[37] N. Sadek, A. Khotanzad, T. Chen. ATM Dynamic Bandwidth Allocation Using F-ARIMA Prediction Model. *Proceedings of ICCCN (International Conference on Computer Communications and Networks)*, pp.359-363, October 20-22, 2003.

[38] Y. Shu, Z. Jin, L. Zhang, L. Wang, O. W. W. Yang. Traffic Prediction Using FARIMA Models. *IEEE International Conference on Communcation*, 2, pp.891-895, 1999.

[39] C. G. Dethe, D. G. Wakde. On the Prediction of Packet Process in Network Traffic Using FARIMA Time-series Model. *Journal of Indian Institute of Science*, 84, pp.31-39, Jan-Apr, 2001.

[40] OPNET (Optimum Network Performance), *http://www.opnet.com.*

[41] Matlab. [onine]. *http://www.matlab.com.*

[42] [onine]. *http://www-tkn.ee.tu-berlin.de/research.*

Appendix

Results of Variance Time Plot Analysis:

Table 1: Speed Scenario of U[0, 20] (m/s)

Table 2: Speed Scenario of U[0, 40] (m/s)

Table 3: Speed Scenario of U[0, 60] (m/s)

Table 4: Speed Scenario of U[0, 80] (m/s)

Table 5: Speed Scenario of U[0, 100] (m/s)

n-n	β	**H**	**r**	**n-n**	β	**H**	**r**	**n-n**	β	**H**	**r**
0-1	-0.056	0.972	0.821	1-0	-0.074	0.963	0.841	2-0	-0.608	0.696	0.975
0-2	-0.629	0.686	0.974	1-2	-0.052	0.974	0.857	2-1	-0.040	0.980	0.890
0-3	-0.008	0.996	0.814	1-3	-0.008	0.996	0.835	2-3	-0.065	0.967	0.851
0-4	-0.014	0.993	0.901	1-4	-0.008	0.996	0.858	2-4	-0.043	0.979	0.881
0-5	-0.095	0.953	0.855	1-5	-0.009	0.995	0.858	2-5	-0.046	0.977	0.873
0-6	-0.015	0.992	0.749	1-6	-0.043	0.978	0.800	2-6	-0.045	0.977	0.864
0-7	-0.014	0.993	0.902	1-7	-0.020	0.990	0.853	2-7	-0.199	0.901	0.891
0-8	-0.026	0.987	0.866	1-8	-0.022	0.989	0.812	2-8	-0.031	0.985	0.915
0-9	-0.072	0.964	0.759	1-9	-0.008	0.996	0.847	2-9	-0.026	0.987	0.812
0-10	-0.319	0.841	0.841	1-10	-0.084	0.958	0.899	2-10	-0.042	0.979	0.885
0-11	-0.009	0.995	0.818	1-11	-0.017	0.991	0.864	2-11	-0.044	0.978	0.901
3-0	-0.031	0.985	0.779	4-0	-0.008	0.996	0.887	5-0	-0.131	0.935	0.845
3-1	-0.022	0.989	0.749	4-1	-0.004	0.998	0.845	5-1	-0.007	0.996	0.874
3-2	-0.039	0.980	0.752	4-2	-0.028	0.986	0.738	5-2	-0.022	0.989	0.782
3-4	-0.022	0.989	0.776	4-3	-0.006	0.997	0.877	5-3	-0.005	0.998	0.883
3-5	-0.025	0.988	0.792	4-5	-0.012	0.994	0.849	5-4	-0.012	0.994	0.842
3-6	-0.028	0.986	0.776	4-6	-0.063	0.969	0.808	5-6	-0.022	0.989	0.816
3-7	-0.034	0.983	0.772	4-7	-0.012	0.994	0.827	5-7	-0.046	0.977	0.822
3-8	-0.016	0.992	0.774	4-8	-0.012	0.994	0.806	5-8	-0.072	0.964	0.714
3-9	-0.033	0.984	0.744	4-9	-0.205	0.897	0.886	5-9	-0.044	0.978	0.838
3-10	-0.019	0.990	0.779	4-10	-0.012	0.994	0.801	5-10	-0.006	0.997	0.870
3-11	-0.018	0.991	0.748	4-11	-0.011	0.995	0.799	5-11	-0.032	0.984	0.778
6-0	-0.016	0.992	0.752	7-0	-0.046	0.977	0.775	8-0	-0.085	0.958	0.747
6-1	-0.038	0.981	0.877	7-1	-0.062	0.969	0.810	8-1	-0.018	0.991	0.795
6-2	-0.008	0.996	0.810	7-2	-0.185	0.907	0.868	8-2	-0.034	0.983	0.857
6-3	-0.014	0.993	0.826	7-3	-0.036	0.982	0.757	8-3	-0.006	0.997	0.837
6-4	-0.059	0.970	0.817	7-4	-0.034	0.983	0.768	8-4	-0.016	0.992	0.838
6-5	-0.015	0.992	0.830	7-5	-0.053	0.974	0.792	8-5	-0.008	0.996	0.846
6-7	-0.018	0.991	0.809	7-6	-0.037	0.982	0.800	8-6	-0.007	0.997	0.865
6-8	-0.016	0.992	0.879	7-8	-0.031	0.985	0.808	8-7	-0.008	0.996	0.871
6-9	-0.111	0.945	0.724	7-9	-0.041	0.979	0.800	8-9	-0.006	0.997	0.883
6-10	-0.350	0.825	0.848	7-10	-0.033	0.984	0.778	8-10	-0.008	0.996	0.822
6-11	-0.010	0.995	0.778	7-11	-0.044	0.978	0.806	8-11	-0.139	0.930	0.866
9-0	-0.072	0.964	0.756	10-0	-0.004	0.998	0.859	11-0	-0.005	0.998	0.847
9-1	-0.012	0.994	0.862	10-1	-0.014	0.993	0.876	11-1	-0.013	0.993	0.857
9-2	-0.024	0.988	0.906	10-2	-0.006	0.997	0.827	11-2	-0.013	0.994	0.838
9-3	-0.042	0.979	0.846	10-3	-0.065	0.968	0.750	11-3	-0.006	0.997	0.854
9-4	-0.225	0.888	0.886	10-4	-0.006	0.997	0.862	11-4	-0.030	0.985	0.783
9-5	-0.073	0.963	0.861	10-5	-0.004	0.998	0.830	11-5	-0.007	0.997	0.824
9-6	-0.015	0.992	0.795	10-6	-0.004	0.998	0.818	11-6	-0.009	0.996	0.806
9-7	-0.012	0.994	0.856	10-7	-0.012	0.994	0.812	11-7	-0.058	0.971	0.797
9-8	-0.106	0.947	0.797	10-8	-0.001	1.000	0.231	11-8	-0.140	0.930	0.863
9-10	-0.060	0.970	0.852	10-9	-0.002	0.999	0.760	11-9	-0.031	0.985	0.827
9-11	-0.027	0.986	0.865	10-11	-0.002	0.999	0.851	11-10	-0.009	0.996	0.860

Table 1: Variance-Time Plot Analysis on data of speed scenario of U[0, 20] (m/s)

n-n	β	**H**	**r**	**n-n**	β	**H**	**r**	**n-n**	β	**H**	**r**
0-1	-0.048	0.976	0.820	1-0	-0.253	0.873	0.909	2-0	0.001	1.000	0.101
0-2	-0.080	0.960	0.833	1-2	-0.240	0.880	0.899	2-1	-0.028	0.986	0.789
0-3	-0.127	0.936	0.845	1-3	-0.232	0.884	0.898	2-3	-0.004	0.998	0.786
0-4	-0.071	0.964	0.832	1-4	-0.236	0.882	0.901	2-4	-0.066	0.967	0.817
0-5	-0.083	0.959	0.846	1-5	-0.745	0.627	0.996	2-5	-0.079	0.960	0.825
0-6	-0.128	0.936	0.847	1-6	-0.232	0.884	0.899	2-6	-0.068	0.966	0.728
0-7	-0.078	0.961	0.833	1-7	-0.232	0.884	0.898	2-7	-0.037	0.981	0.891
0-8	-0.080	0.960	0.825	1-8	-0.238	0.881	0.901	2-8	-0.078	0.961	0.838
0-9	-0.077	0.961	0.830	1-9	-0.232	0.884	0.898	2-9	-0.147	0.927	0.793
0-10	-0.093	0.954	0.829	1-10	-0.040	0.980	0.874	2-10	-0.672	0.664	0.978
0-11	-0.098	0.951	0.832	1-11	-0.232	0.884	0.898	2-11	-0.032	0.984	0.861
3-0	-0.040	0.980	0.835	4-0	-0.421	0.790	0.902	5-0	-0.233	0.884	0.844
3-1	-0.030	0.985	0.778	4-1	-0.420	0.790	0.899	5-1	-0.367	0.816	0.990
3-2	-0.005	0.997	0.809	4-2	-0.423	0.788	0.899	5-2	-0.241	0.880	0.829
3-4	-0.031	0.984	0.776	4-3	-0.420	0.790	0.899	5-3	-0.172	0.914	0.891
3-5	-0.262	0.869	0.900	4-5	-0.277	0.861	0.857	5-4	-0.177	0.912	0.903
3-6	-0.016	0.992	0.834	4-6	-0.420	0.790	0.889	5-6	-0.175	0.912	0.848
3-7	-0.017	0.991	0.869	4-7	-0.053	0.973	0.782	5-7	-0.203	0.899	0.888
3-8	-0.023	0.988	0.866	4-8	-0.243	0.879	0.890	5-8	-0.197	0.902	0.885
3-9	-0.005	0.997	0.850	4-9	-0.422	0.789	0.899	5-9	-0.175	0.913	0.896
3-10	-0.021	0.990	0.818	4-10	-0.429	0.786	0.890	5-10	-0.090	0.955	0.897
3-11	-0.062	0.969	0.780	4-11	-0.420	0.790	0.899	5-11	-0.237	0.881	0.833
6-0	-0.031	0.985	0.789	7-0	-0.010	0.995	0.881	8-0	-0.303	0.848	0.890
6-1	-0.146	0.927	0.857	7-1	-0.024	0.988	0.873	8-1	-0.303	0.848	0.895
6-2	-0.054	0.973	0.752	7-2	-0.025	0.988	0.890	8-2	-0.304	0.848	0.890
6-3	-0.010	0.995	0.838	7-3	-0.020	0.990	0.907	8-3	-0.302	0.849	0.892
6-4	-0.027	0.986	0.817	7-4	-0.009	0.996	0.849	8-4	-0.312	0.844	0.902
6-5	-0.027	0.987	0.816	7-5	-0.039	0.981	0.770	8-5	-0.303	0.849	0.891
6-7	-0.453	0.773	0.943	7-6	-0.444	0.778	0.942	8-6	-0.302	0.849	0.894
6-8	-0.017	0.991	0.872	7-8	-0.010	0.995	0.818	8-7	-0.252	0.874	0.856
6-9	-0.015	0.993	0.782	7-9	-0.013	0.994	0.800	8-9	-0.302	0.849	0.891
6-10	-0.707	0.647	0.982	7-10	-0.003	0.999	0.838	8-10	-0.106	0.947	0.877
6-11	-0.019	0.991	0.852	7-11	-0.009	0.995	0.841	8-11	-0.303	0.849	0.891
9-0	-0.110	0.945	0.785	10-0	-0.272	0.864	0.793	11-0	-0.037	0.982	0.844
9-1	-0.053	0.973	0.879	10-1	-0.243	0.878	0.780	11-1	-0.070	0.965	0.893
9-2	-0.151	0.925	0.825	10-2	-0.434	0.783	0.934	11-2	-0.087	0.957	0.843
9-3	-0.052	0.974	0.944	10-3	-0.267	0.866	0.784	11-3	-0.062	0.969	0.781
9-4	0.029	1.015	0.286	10-4	-0.276	0.862	0.795	11-4	-0.091	0.955	0.839
9-5	-0.630	0.685	0.972	10-5	-0.200	0.900	0.794	11-5	-0.063	0.969	0.693
9-6	-0.019	0.990	0.781	10-6	-0.390	0.805	0.912	11-6	-0.016	0.992	0.824
9-7	-0.082	0.959	0.849	10-7	-0.059	0.971	0.791	11-7	-0.065	0.968	0.874
9-8	-0.016	0.992	0.895	10-8	-0.264	0.868	0.777	11-8	-0.022	0.989	0.840
9-10	-0.015	0.993	0.783	10-9	-0.128	0.936	0.808	11-9	-0.014	0.993	0.796
9-11	-0.077	0.961	0.829	10-11	-0.264	0.868	0.777	11-10	-0.019	0.990	0.792

Table 2: Variance-Time Plot Analysis on data of speed scenario of U[0, 40] (m/s)

n-n	β	**H**	**r**	**n-n**	β	**H**	**r**	**n-n**	β	**H**	**r**
0-1	-0.067	0.966	0.859	1-0	-0.089	0.955	0.826	2-0	-0.015	0.992	0.839
0-2	-0.020	0.990	0.829	1-2	-0.593	0.703	0.980	2-1	-0.584	0.708	0.978
0-3	-0.149	0.925	0.793	1-3	-0.143	0.929	0.877	2-3	-0.585	0.708	0.970
0-4	-0.006	0.997	0.657	1-4	-0.265	0.868	0.894	2-4	-0.177	0.912	0.880
0-5	-0.295	0.852	0.914	1-5	-0.025	0.988	0.808	2-5	-0.036	0.982	0.786
0-6	-0.017	0.991	0.838	1-6	-0.018	0.991	0.837	2-6	-0.112	0.944	0.794
0-7	-0.009	0.995	0.859	1-7	-0.275	0.863	0.911	2-7	-0.087	0.956	0.865
0-8	-0.008	0.996	0.894	1-8	-0.014	0.993	0.814	2-8	-0.109	0.945	0.626
0-9	-0.017	0.991	0.871	1-9	-0.070	0.965	0.828	2-9	-0.047	0.976	0.768
0-10	-0.060	0.970	0.756	1-10	-0.034	0.983	0.807	2-10	-0.039	0.980	0.834
0-11	-0.015	0.992	0.834	1-11	-0.032	0.984	0.794	2-11	-0.043	0.978	0.923
3-0	-0.144	0.928	0.815	4-0	-0.238	0.881	0.940	5-0	-0.056	0.972	0.781
3-1	-0.027	0.987	0.894	4-1	-0.128	0.936	0.802	5-1	-0.070	0.965	0.758
3-2	-0.590	0.705	0.969	4-2	-0.173	0.913	0.907	5-2	-0.054	0.973	0.779
3-4	-0.038	0.981	0.786	4-3	-0.101	0.950	0.827	5-3	-0.056	0.972	0.781
3-5	-0.016	0.992	0.791	4-5	-0.116	0.942	0.848	5-4	-0.053	0.973	0.771
3-6	-0.035	0.982	0.905	4-6	-0.264	0.868	0.890	5-6	-0.055	0.973	0.774
3-7	-0.002	0.999	0.275	4-7	-0.167	0.916	0.879	5-7	-0.054	0.973	0.775
3-8	-0.012	0.994	0.863	4-8	-0.133	0.934	0.866	5-8	-0.054	0.973	0.777
3-9	-0.008	0.996	0.874	4-9	-0.759	0.620	0.991	5-9	-0.043	0.979	0.783
3-10	-0.007	0.997	0.910	4-10	-0.105	0.947	0.848	5-10	-0.056	0.972	0.773
3-11	-0.011	0.995	0.900	4-11	-0.229	0.885	0.905	5-11	-0.031	0.985	0.830
6-0	-0.182	0.909	0.771	7-0	-0.358	0.821	0.925	8-0	-0.008	0.996	0.828
6-1	-0.190	0.905	0.772	7-1	-0.174	0.913	0.827	8-1	-0.008	0.996	0.540
6-2	-0.183	0.908	0.770	7-2	-0.236	0.882	0.883	8-2	-0.087	0.956	0.780
6-3	-0.182	0.909	0.771	7-3	-0.070	0.965	0.899	8-3	-0.019	0.991	0.823
6-4	-0.182	0.909	0.794	7-4	-0.443	0.778	0.947	8-4	-0.015	0.992	0.803
6-5	-0.032	0.984	0.859	7-5	-0.299	0.851	0.929	8-5	-0.029	0.986	0.790
6-7	-0.183	0.909	0.771	7-6	-0.183	0.908	0.810	8-6	-0.007	0.997	0.895
6-8	-0.022	0.989	0.755	7-8	-0.165	0.918	0.851	8-7	-0.067	0.967	0.757
6-9	-0.184	0.908	0.770	7-9	-0.347	0.826	0.920	8-9	-0.024	0.988	0.547
6-10	-0.176	0.912	0.775	7-10	-0.182	0.909	0.824	8-10	-0.009	0.996	0.813
6-11	-0.182	0.909	0.772	7-11	-0.170	0.915	0.806	8-11	-0.005	0.998	0.691
9-0	-0.311	0.844	0.889	10-0	-0.028	0.986	0.778	11-0	-0.020	0.990	0.828
9-1	-0.260	0.870	0.859	10-1	-0.012	0.994	0.844	11-1	-0.459	0.771	0.932
9-2	-0.303	0.848	0.894	10-2	-0.064	0.968	0.803	11-2	-0.037	0.982	0.232
9-3	-0.139	0.930	0.844	10-3	0.003	1.001	0.177	11-3	0.003	1.002	0.087
9-4	-0.611	0.695	0.974	10-4	-0.805	0.598	0.991	11-4	-0.127	0.937	0.886
9-5	-0.124	0.938	0.900	10-5	-0.025	0.988	0.799	11-5	-0.008	0.996	0.871
9-6	-0.331	0.835	0.889	10-6	-0.008	0.996	0.824	11-6	0.010	1.005	0.233
9-7	-0.461	0.769	0.945	10-7	-0.220	0.890	0.885	11-7	-0.003	0.998	0.170
9-8	-0.304	0.848	0.889	10-8	-0.008	0.996	0.839	11-8	-0.004	0.998	0.194
9-10	-0.301	0.850	0.890	10-9	-0.010	0.995	0.817	11-9	-0.015	0.993	0.813
9-11	-0.300	0.850	0.887	10-11	-0.051	0.975	0.754	11-10	-0.037	0.981	0.783

Table 3: Variance-Time Plot Analysis on data of speed scenario of U[0, 60] (m/s)

n-n	β	**H**	**r**	**n-n**	β	**H**	**r**	**n-n**	β	**H**	**r**
0-1	-0.107	0.946	0.907	1-0	-0.103	0.948	0.746	2-0	-0.087	0.957	0.857
0-2	-0.103	0.948	0.841	1-2	-0.034	0.983	0.779	2-1	-0.034	0.983	0.787
0-3	-0.068	0.966	0.748	1-3	-0.029	0.985	0.722	2-3	-0.067	0.966	0.845
0-4	-0.138	0.931	0.812	1-4	-0.091	0.955	0.795	2-4	-0.998	0.501	1.000
0-5	-0.078	0.961	0.768	1-5	-0.063	0.969	0.859	2-5	-0.038	0.981	0.765
0-6	-0.466	0.767	0.953	1-6	-0.122	0.939	0.878	2-6	-0.015	0.992	0.858
0-7	-0.025	0.988	0.803	1-7	-0.469	0.765	0.927	2-7	-0.062	0.969	0.790
0-8	-0.178	0.911	0.885	1-8	-0.044	0.978	0.864	2-8	-0.061	0.970	0.811
0-9	-0.204	0.898	0.817	1-9	-0.075	0.963	0.729	2-9	-0.028	0.986	0.952
0-10	-0.146	0.927	0.908	1-10	-0.181	0.910	0.879	2-10	-0.072	0.964	0.810
0-11	-0.064	0.968	0.670	1-11	-0.045	0.977	0.850	2-11	-0.011	0.994	0.834
3-0	-0.085	0.958	0.829	4-0	-0.057	0.971	0.766	5-0	-0.100	0.950	0.775
3-1	-0.200	0.900	0.741	4-1	-0.086	0.957	0.775	5-1	-0.108	0.946	0.732
3-2	-0.195	0.902	0.737	4-2	-0.976	0.512	1.000	5-2	-0.123	0.938	0.782
3-4	-0.197	0.901	0.737	4-3	-0.086	0.957	0.844	5-3	-0.110	0.945	0.737
3-5	-0.047	0.977	0.870	4-5	-0.131	0.935	0.834	5-4	-0.182	0.909	0.886
3-6	-0.196	0.902	0.738	4-6	-0.040	0.980	0.874	5-6	-0.107	0.946	0.729
3-7	-0.183	0.909	0.740	4-7	-0.040	0.980	0.818	5-7	-0.111	0.944	0.743
3-8	-0.196	0.902	0.740	4-8	-0.037	0.981	0.907	5-8	-0.119	0.941	0.766
3-9	-0.204	0.898	0.745	4-9	-0.034	0.983	0.767	5-9	-0.037	0.981	0.706
3-10	-0.221	0.890	0.772	4-10	-0.331	0.835	0.924	5-10	-0.206	0.897	0.908
3-11	-0.196	0.902	0.737	4-11	-0.040	0.980	0.816	5-11	-0.121	0.940	0.775
6-0	-0.465	0.768	0.953	7-0	-0.010	0.995	0.877	8-0	-0.025	0.987	0.823
6-1	-0.361	0.819	0.925	7-1	-0.371	0.814	0.922	8-1	-0.092	0.954	0.823
6-2	-0.066	0.967	0.869	7-2	-0.018	0.991	0.922	8-2	-0.301	0.849	0.860
6-3	-0.210	0.895	0.876	7-3	-0.012	0.994	0.927	8-3	-0.019	0.991	0.896
6-4	-0.053	0.973	0.853	7-4	-0.021	0.989	0.927	8-4	-0.082	0.959	0.918
6-5	-0.089	0.956	0.869	7-5	-0.016	0.992	0.920	8-5	-0.063	0.969	0.887
6-7	-0.107	0.947	0.872	7-6	-0.017	0.992	0.802	8-6	-0.014	0.993	0.902
6-8	-0.027	0.986	0.868	7-8	-0.022	0.989	0.899	8-7	-0.019	0.991	0.857
6-9	-0.089	0.955	0.825	7-9	-0.136	0.932	0.774	8-9	-0.066	0.967	0.874
6-10	-0.094	0.953	0.848	7-10	-0.009	0.995	0.905	8-10	-0.027	0.986	0.842
6-11	-0.069	0.966	0.879	7-11	-0.094	0.953	0.889	8-11	-0.029	0.986	0.821
9-0	-0.115	0.943	0.808	10-0	-0.024	0.988	0.795	11-0	-0.008	0.996	0.753
9-1	-0.106	0.947	0.819	10-1	-0.186	0.907	0.873	11-1	-0.025	0.987	0.792
9-2	-0.075	0.962	0.838	10-2	-0.015	0.993	0.838	11-2	-0.038	0.981	0.817
9-3	-0.076	0.962	0.837	10-3	-0.010	0.995	0.869	11-3	-0.021	0.989	0.828
9-4	-0.035	0.982	0.899	10-4	-0.450	0.775	0.938	11-4	-0.042	0.979	0.814
9-5	-0.033	0.984	0.823	10-5	-0.339	0.830	0.922	11-5	-0.026	0.987	0.812
9-6	-0.050	0.975	0.821	10-6	-0.030	0.985	0.862	11-6	-0.024	0.988	0.833
9-7	-0.029	0.985	0.844	10-7	-0.014	0.993	0.823	11-7	-0.101	0.949	0.792
9-8	-0.036	0.982	0.843	10-8	-0.013	0.993	0.822	11-8	-0.029	0.985	0.835
9-10	-0.043	0.978	0.729	10-9	-0.041	0.979	0.719	11-9	-0.065	0.968	0.804
9-11	-0.034	0.983	0.839	10-11	-0.040	0.980	0.824	11-10	-0.013	0.993	0.822

Table 4: Variance-Time Plot Analysis on data of speed scenario of U[0, 80] (m/s)

n-n	β	**H**	**r**	**n-n**	β	**H**	**r**	**n-n**	β	**H**	**r**
0-1	-0.044	0.978	0.915	1-0	-0.046	0.977	0.825	2-0	-0.070	0.965	0.815
0-2	-0.038	0.981	0.898	1-2	-0.033	0.984	0.902	2-1	-0.012	0.994	0.920
0-3	-0.061	0.970	0.901	1-3	-0.051	0.974	0.726	2-3	-0.141	0.930	0.905
0-4	-0.027	0.987	0.911	1-4	-0.071	0.965	0.905	2-4	-0.577	0.712	0.965
0-5	-0.043	0.978	0.923	1-5	-0.072	0.964	0.877	2-5	-0.686	0.657	0.979
0-6	-0.043	0.978	0.919	1-6	-0.053	0.973	0.811	2-6	-0.053	0.973	0.833
0-7	-0.044	0.978	0.922	1-7	-0.048	0.976	0.834	2-7	-0.034	0.983	0.892
0-8	-0.045	0.978	0.926	1-8	-0.076	0.962	0.875	2-8	-0.117	0.941	0.854
0-9	-0.055	0.973	0.924	1-9	-0.129	0.936	0.886	2-9	-0.038	0.981	0.867
0-10	-0.046	0.977	0.910	1-10	-0.065	0.967	0.806	2-10	-0.024	0.988	0.876
0-11	-0.044	0.978	0.926	1-11	-0.093	0.953	0.847	2-11	-0.016	0.992	0.933
3-0	-0.055	0.972	0.821	4-0	-0.335	0.833	0.890	5-0	-0.049	0.976	0.824
3-1	-0.092	0.954	0.783	4-1	-0.436	0.782	0.941	5-1	-0.039	0.981	0.753
3-2	-0.162	0.919	0.926	4-2	-0.220	0.890	0.921	5-2	-0.028	0.986	0.703
3-4	-0.063	0.968	0.851	4-3	-0.333	0.833	0.889	5-3	-0.035	0.983	0.752
3-5	-0.061	0.969	0.829	4-5	-0.373	0.813	0.923	5-4	-0.179	0.910	0.973
3-6	-0.102	0.949	0.916	4-6	-0.331	0.834	0.889	5-6	-0.987	0.506	1.000
3-7	-0.058	0.971	0.875	4-7	-0.334	0.833	0.890	5-7	-0.028	0.986	0.704
3-8	-0.079	0.960	0.816	4-8	-0.190	0.905	0.837	5-8	-0.037	0.981	0.740
3-9	-0.071	0.965	0.891	4-9	-0.335	0.833	0.891	5-9	-0.017	0.991	0.772
3-10	-0.061	0.970	0.849	4-10	-0.030	0.985	0.905	5-10	-0.033	0.983	0.720
3-11	-0.050	0.975	0.856	4-11	-0.332	0.834	0.889	5-11	-0.108	0.946	0.960
6-0	-0.044	0.978	0.715	7-0	-0.058	0.971	0.880	8-0	-0.151	0.924	0.908
6-1	-0.056	0.972	0.758	7-1	-0.049	0.976	0.753	8-1	-0.173	0.913	0.922
6-2	-0.039	0.981	0.678	7-2	-0.056	0.972	0.700	8-2	-0.116	0.942	0.866
6-3	-0.055	0.972	0.752	7-3	-0.046	0.977	0.792	8-3	-0.110	0.945	0.899
6-4	-0.022	0.989	0.666	7-4	-0.065	0.968	0.811	8-4	-0.071	0.964	0.755
6-5	-0.990	0.505	1.000	7-5	-0.045	0.978	0.728	8-5	-0.211	0.894	0.914
6-7	-0.043	0.978	0.691	7-6	-0.035	0.982	0.845	8-6	-0.148	0.926	0.917
6-8	-0.043	0.978	0.681	7-8	-0.080	0.960	0.875	8-7	-0.094	0.953	0.843
6-9	-0.049	0.975	0.651	7-9	-0.782	0.609	0.991	8-9	-0.290	0.855	0.911
6-10	-0.053	0.974	0.761	7-10	-0.051	0.975	0.860	8-10	-0.062	0.969	0.844
6-11	-0.045	0.978	0.670	7-11	-0.049	0.976	0.769	8-11	-0.068	0.966	0.813
9-0	-0.503	0.749	0.907	10-0	-0.028	0.986	0.903	11-0	-0.053	0.973	0.882
9-1	-0.370	0.815	0.946	10-1	-0.019	0.991	0.831	11-1	-0.106	0.947	0.917
9-2	-0.110	0.945	0.920	10-2	-0.011	0.994	0.892	11-2	-0.047	0.977	0.873
9-3	-0.492	0.754	0.912	10-3	-0.361	0.820	0.911	11-3	-0.042	0.979	0.837
9-4	-0.506	0.747	0.910	10-4	-0.145	0.928	0.833	11-4	-0.043	0.979	0.867
9-5	-0.505	0.747	0.906	10-5	-0.303	0.848	0.923	11-5	-0.302	0.849	0.987
9-6	-0.285	0.858	0.851	10-6	-0.037	0.981	0.811	11-6	-0.056	0.972	0.882
9-7	-0.809	0.596	0.990	10-7	-0.262	0.869	0.883	11-7	-0.051	0.975	0.882
9-8	-0.514	0.743	0.906	10-8	-0.682	0.659	0.972	11-8	-0.056	0.972	0.881
9-10	-0.304	0.848	0.932	10-9	-0.376	0.812	0.944	11-9	-0.077	0.961	0.888
9-11	-0.507	0.747	0.905	10-11	-0.024	0.988	0.825	11-10	-0.059	0.970	0.895

Table 5: Variance-Time Plot Analysis on data of speed scenario of U[0, 100] (m/s)